Tetrahedron Vol. 48, No. 4, pp. 695-718, 1992
Printed in Great Britain

0040-4020/92 $3.00+.00

Assessment of Competing 2'→5' versus 3'→5' Stackings in Solution Structure of Branched-RNA by ^{1}H- & ^{31}P-NMR Spectroscopy

Christian Sund, Peter Agback, Leo H. Koole, Anders Sandström & Jyoti Chattopadhyaya*

Department of Bioorganic Chemistry, Box 581, Biomedical Center,
University of Uppsala, S-751 23 Uppsala, Sweden

(*Received in UK* 18 *November* 1991)

Abstract: *Preparation of five novel phosphorylated derivatives of adenosine, i.e. adenosine 2',3'-bis(ethylphosphate) (**11**), adenosine 2',3'-bis(phosphate) (**13**), adenosine 2',3',5'-tris(ethylphosphate) (**15**), adenosine 2',5'-bis(ethylphosphate) (**17**), and adenosine 3',5'-bis(ethylphosphate) (**19**) is reported. These compounds, along with methyl β-D-ribofuranosyl-bis-2',3'-ethylphosphate (**9**), were used as reference systems for ^{31}P and ^{1}H-NMR conformational studies on the branched RNA structures **20** - **30**. Compounds **11**, **13**, **15**, **17**, and **19** preserve the essential structural elements of the branch point adenosine, while the intramolecular base stacking interactions are removed. The ^{31}P-NMR chemical shifts of **20** - **30**, referenced against **9**, **11**, **13**, or **15**, show a pattern that is generally consistent with our previous results from variable temperature ^{31}P-NMR experiments. The data indicate that the contribution of g,g around the P-O3' (ζ) and P-O5' (α) bonds is significantly greater for the 2'-phosphate group than for the 3'-phosphate group. These results point towards preferential 2'→5' rather than 3'→5' base stacked structures in all of these synthetic models of the lariat. This is especially the case for the branched trimer **20** and the pentamer **27** which are part of a naturally occurring lariat structure. Note that the strongest 2'→5' stacking is however found in the unnatural trimers **22** and **23** in which the 2'-linked residue is a pyrimidine nucleotide. Compounds **11**, **13**, and **15** were also used to calibrate the ^{1}H-NMR oligomerization shifts of the H2 protons of the branch-point adenosine. These data show a consistency with the results from variable temperature ^{1}H-NMR experiments, as well as with the results of ^{31}P-NMR experiments. The results obtained with the series of compounds **20** ($A^{2'p5'G}_{3'p5'U}$), **26a** ($UA^{2'p5'G}_{3'p5'U}$), **27** ($A^{2'p5'GU}_{3'p5'UC}$), **28** ($CUA^{2'p5'GU}_{3'p5'UC}$), **29** ($CUA^{2'p5'GUG}_{3'p5'UCA}$), and **30** ($CCUA^{2'p5'GUG}_{3'p5'UCA}$) are of special interest since these structures are constituents of the naturally occurring lariat in the excised intron in Group II splicing of bl 1 of Yeast mitochondria. Qualitatively, the present ^{1}H- and ^{31}P-NMR data on **26a**, **27**, **28**, **29**, and **30** show 2'→5' base stacking of an intermediate strength; 2'→5' base stacking is substantially stronger for trimer **20** and pentamer **27**. This difference is ascribed to the 5'-conformational transmission effect owing to the presence of at least one nucleotide upstream of the branch-point. 5'-Conformational transmission appears to weaken the 2'→5' stacking at the expense of some 3'→5' stacking. The experimental data on the conformation of **20** ($A^{2'p5'G}_{3'p5'U}$) (^{31}P and ^{1}H chemical shifts, vicinal ^{1}H-^{1}H, ^{1}H-^{31}P, and ^{13}C-^{31}P coupling constants) formed the basis for a series of AMBER molecular mechanics calculations. These molecular modelling studies allowed us to conclude that g,g conformation in the 2'-phosphate group is primarily g⁻(ζ),g⁻(α). This is found to be the only conformation that gives 2'→5' base stacking as evident in the temperature dependent chemical shift and in the oligomerization shift studies. Modelling studies furthermore showed two energetically possible ζ and α torsions for the 3'-phosphate group (g⁻(ζ),g⁻(α) and g⁻(ζ),t(α)). The present use of reference compounds **9**, **11**, **13**, **15**, **17**, and **19** has led to a refined and partially revised concept for the conformational description of oligomeric branched RNAs.*

The tertiary structure of nucleic acids is stabilized to a large extent by vertical base-base interactions, usually referred to as base stacking.[1] Base stacking probably originates from dipole-dipole interactions

between polarized groups (e.g. C=O, NH_2), and polarizable clouds of π-electrons.[2] Much of our current knowledge on base stacking originates from crystal structural studies on oligonucleotides.[1b] There is a vast body of spectroscopic evidence that the intramolecular base stacking is usually preserved for oligonucleotides in aqueous solution.[1c] Dinucleoside monophosphates of the type X3'p5'Y obviously form the simplest systems to study intramolecular base stacking in solution. Thermodynamic data concerning the stack ⇄ destack equilibria have been measured by different techniques, and for different nucleoside bases X and Y. It has been established that the propensity to stack is in the order purine-3'p5'-purine > purine-3'p5'-pyrimidine ≈ pyrimidine-3'p5'-purine > pyrimidine-3'p5'-pyrimidine.[1b] Much less is known, however, about stacking in dinucleoside monophosphates of the type X2'p5'Y. Crystal structures of A(N^1H^+)2'p5'U,[3] A2'p5'C(N^3H^+),[4] and C(N^3H^+)2'p5'A[5] have been reported in the literature. Analysis of A(N^1H^+)2'p5'U and A2'p5'C(N^3H^+) show the stacking between the ribose oxygen O4' and adenine; the purine is *anti* in the former,[3] and *syn* in the latter.[4] In both A(N^1H^+)2'p5'U and A2'p5'C(N^3H^+), the furanose puckering is C2'-*endo*, C3'-*endo*. On the other hand, in C(N^3H^+)2'p5'A,[5] the furanose conformation is C3'-*endo*, C2'-*endo* and it forms miniature righthanded double helix having 2'→5'-linked parallel strands. The two bases in these 2'→5'-linked dimers are oriented parallel to each other but there seems to be an absense of intramolecular base stacking in contrast with the solution studies wherein 2'→5' base stacking is clearly established.[6] It is by no means certain, however, that the stack propensities of different combinations of purine and pyrimidine bases are the same for 2'→5' and 3'→5' dinucleotides.

In view of the above, it is of interest to examine the nature of base stacking in branched RNA oligomers of the type $X^{2'p5'Y}_{3'p5'Z}$. *A priori*, these systems can show 2'→5' as well as 3'→5' base stacking. There is much current interest in branched RNA structures, because of their occurrence in lariat type excised introns in Group II or nuclear mRNA splicing.[7-9,12] Preferred 2'→5' over 3'→5' base stacking has been reported for a variety of branched RNA trimers studied in aqueous solution.[7c,i,j,m,n,9] Several lines of evidence led to this conclusion: (i) spectroscopic (^{1}H-NMR,[7c,i,j,m,n] temperature-dependent ^{31}P-NMR shifts,[7m] and circular dichroism[7j,n]) comparisons of trimers $X^{2'p5'Y}_{3'p5'Z}$ with the constituent dimers X2'p5'Y and X3'p5'Z showed a close correspondence between the trimers and the 2'→5' dimers[7c]; these comparisons also comprised chemical shift (δ) versus temperature profiles. (ii) it was observed that the δ-values of the branch-point residue are influenced by the 2'-residue, and vice versa, while the δ-values of the 3'-residue are virtually independent of the nature of the branch-point and the 2'-residue. (iii) the magnetic inequivalence of H5' and H5", if compared to the 5'-phosphorylated monomers, is larger for the 2'-residues than for the 3'-residues,[9a] (iv) the observation that the C3'-O3' (ε) bond resides mainly as the ε⁻ rotamer,[7p] which seems to prohibit 3'→5' stacking.[9a] A preference of 2'→5' over 3'→5' base stacking, i.e. a conformation in which the 3'-residue is essentially free, is found regardless of the nature of the 2'-residue. It should be noted, however, that no clear conclusions could be drawn about the mode of base-base stacking in branched trimers in which either cytidine or uridine forms the branch-point.[7n] Discrimination between 2'→5' and 3'→5' base stacking was almost exclusively based on comparisons with structural constituents. Obviously, this is a cumbersome approach, especially if one wants to study the conformation of branched RNAs beyond the trimer level. To address this problem, we have now studied whether the ^{1}H and ^{31}P NMR *oligomeric shifts* of the H2A and 2'- and 3'-phosphates can be used to identify which mode of stacking is operative. This means that the ^{1}H and ^{31}P NMR chemical shifts of the oligomer are compared with those of the monomeric constituents *at the same temperature*. The reason for the

choice of H2A of the branch-point adenine moiety as a a neutral marker for assessing the base-stacking with neighbouring nucleobases is that it is remotely located from the O4' of pentose sugar and the 5'-phosphate. On the other hand, ^{31}P chemical shifts constitute an independent and complementary marker of the phosphate-ester conformation in nucleic acids as was pointed out by Gorenstein.[7m,n, 22] We realized that a comparative study of ^{1}H and ^{31}P chemical shifts within a series of branched RNAs requires a *ubiquitous reference system.* Clearly, the requirement for such a *ubiquitous reference system* demands that the effect of intramolecular base stacking interactions are eliminated with the preservation of all other structural elements. To this end, we have synthesized compounds **9** [methyl β-D-ribofuranosyl-2',3'-bis(ethylphosphate)], **11** [adenosine 2',3'-bis(ethylphosphate)], **13** [adenosine 2',3'-bis(phosphate)], **15** [adenosine 2',3',5'-tris(ethylphosphate)], **17** [adenosine 2',5'-bis(ethylphosphate)], and **19** [adenosine 3',5'-bis(ethylphosphate)] in order to examine which of these compounds can serve best for this purpose. Use of either **9**, **11**, **13**, or **15** as reference systems confirmed the preference for 2'→5' over 3'→5' base stacking in a series of trimeric[7c,i,j,m,n], tetrameric[7,e,k], penta- and heptameric[7g,s], and nona- and decameric[7n] branched-RNA which model the lariat formed in the penultimate step of the ligation of two exons in the Group II mRNA splicing of intron. Hence it is concluded that these four reference compounds provide a new independent tool for conformational analysis of branched RNAs. Furthermore, we report a comparative conformational analysis of reference compounds **9**, **11**, **13**, **15**, **17** and **19**, based on vicinal ^{1}H - ^{1}H, ^{1}H - ^{13}C, and ^{1}H - ^{31}P coupling constants.

RESULTS AND DISCUSSION

Preparation of the reference compounds 9, 11, 13, 15, 17 & 19. Synthesis of symmetrical 2',3'-bis(phosphotriester), 2',3'-bis(phosphodiester) and 2',3'-bis(phosphomonoester) derivatives of nucleosides requires a highly reactive phosphorylating or phosphitylating species in order to avoid the formation of 2',3'-cyclic phosphate due to the neighbouring group participation of the vicinal diol system in a ribonucleoside. Certain P(III) species such as (dialkoxy)-(N,N-dialkylamino)phosphines and alkyl-N,N-dialkyl phosphoramido chloridites meet this requirement. In the synthesis of 2′,3′-symmetrical branched trimers[10-12], the ribonucleoside 2′,3′-bis(phosphotriester) and 2′,3′-bis(phosphodiester) linkages have been introduced by reacting an appropriately protected 2′,3′-dihydroxy ribonucleoside with an appropriately protected 5′-phosphoramidite of a ribonucleoside[11,12] in presence of an activating agent. Alternatively, the reaction of the 2′,3′-dihydroxy ribonucleoside block with 2-cyanoethyl-(or methyl-)-N,N-diiso propylphosphoramido chloridite gives the corresponding 2′,3′-bis(phosphoramidite) which is then coupled to the 5′-hydroxy function of an appropriately protected ribonucleoside block[11]. For the synthesis of O-alkyl phosphate*monoesters*, a procedure was developed by Yoshikawa *et al* [13] using neat $POCl_3$ at low temperatures. An N-phosphoryl-N′-methylimidazolium salt was also used by Takaku *et al* [14] for the same purpose. Furthermore, a number of phosphotriester functions with easily removable protecting groups have been introduced in order to generate O-alkyl phosphates, such as the (O-alkyl)-dibenzylphosphotriester[15], (O-alkyl)-diallylphosphotriester[16], (O-alkyl)-bis[(2-cyanoethyl)phosphotriester][17], (O-alkyl)-bis(t-butyl)phospho triester[18], (O-alkyl)-O-aryl-S-methyl phosphorothioate[19] and the (O-alkyl)-phosphoro-bis(anilidate)[20] functions. However, all these phosphorylating agents have only been used to give 3'- or 5'-phosphomonoester. In our present work, we have successfully used (bis(2-cyanoethoxy))-(N,N-diisopropylamino)phosphine **7** for the synthesis of the adenosine 2′,3′-*bis(phosphomonoester)* **13**. Earlier, Bannwarth *et al.*[17] introduced **7** for their synthesis of 5′-phosphomonoesters of DNA and phosphomonoesters

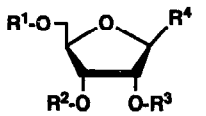

1 : $R^1 = R^2 = R^3 = H$, $R^4 = A^{Bz}$
2 : $R^1 = R^2 = H$, $R^3 = Pix$, $R^4 = A^{Bz}$
3 : $R^1 = R^3 = H$, $R^2 = TBDMS$, $R^4 = A^{Bz}$
4 : $R^1 = DMTr$, $R^2 = R^3 = H$, $R^4 = A^{Bz}$
5 : $R^1 = Fmoc$, $R^2 = R^3 = H$, $R^4 = OMe$

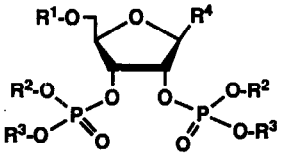

8 : $R^1 = Fmoc$, $R^2 = Et$, $R^3 = Ce$, $R^4 = OMe$
9 : $R^1 = H$, $R^2 = Et$, $[O\text{-}R^3] = [O^- Na^+]$, $R^4 = OMe$
10 : $R^1 = DMTr$, $R^2 = Et$, $R^3 = Ce$, $R^4 = A^{Bz}$
11 : $R^1 = H$, $R^2 = Et$, $[O\text{-}R^3] = [O^- Na^+]$, $R^4 = A$
12 : $R^1 = DMTr$, $R^2 = R^3 = Ce$, $R^4 = A^{Bz}$
13 : $R^1 = H$, $[O\text{-}R^2] = [O\text{-}R^3] = [O^- Na^+]$, $R^4 = A$

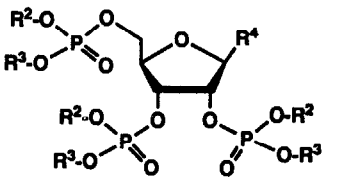

14 : $R^2 = Et$, $R^3 = Ce$, $R^4 = A^{Bz}$
15 : $R^2 = Et$, $[O\text{-}R^3] = [O^- Na^+]$, $R^4 = A$

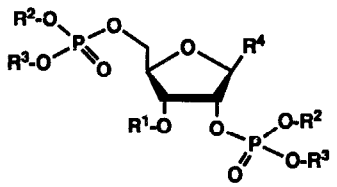

16 : $R^1 = TBDMS$, $R^2 = Et$, $R^3 = Ce$, $R^4 = A^{Bz}$
17 : $R^1 = H$, $R^2 = Et$, $[O\text{-}R^3] = [O^- Na^+]$, $R^4 = A$

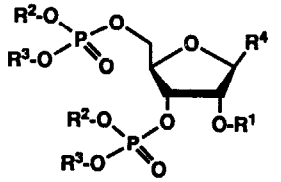

18 : $R^1 = Pix$, $R^2 = Et$, $R^3 = Ce$, $R^4 = A^{Bz}$
19 : $R^1 = H$, $R^2 = Et$, $[O\text{-}R^3] = [O^- Na^+]$, $R^4 = A$

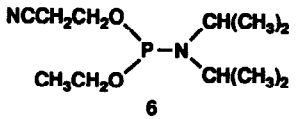

6

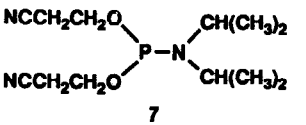

7

Abbrevations: Fmoc = fluorenmethoxycarbonyl; DMTr = 4,4′-dimethoxytrityl; Pix = 9-phenylxanthen-9-yl; TBDMS = t-butyldimethylsilyl; Ce = 2-cyanoethyl; Et = ethyl; Me = methyl; A^{Bz} = N^6-benzoyl-9-adeninyl; A = 9-adeninyl;

of oligopeptides. For the synthesis of the target O-ethyl phosphodiester analogues **9, 11, 15, 17** and **19**, we have employed (2-cyanoethoxy)-(ethoxy)-(N,N-diisopropylamino)phosphine **6** as a reagent for the first time. Reagent **6** was prepared in a similar manner as described for **7**[17], using ethanol instead of 2-cyanoethanol in the second reaction step, and was isolated by silica gel chromatography in 76% yield (δ ^{31}P = +146.89) as a colorless oil. This reagent was then used for phosphorylation of blocks **1-5** according to the procedure described earlier[7h] (5 eq of **6** and 15 eq of tetrazole for each hydroxyl function in the substrate). The reactions were carried out in DMF-MeCN solution at room temperature under argon and standard aqueous iodine oxidation of the intermediary phosphite triesters gave the corresponding phosphotriesters: **1+6** → **14** (80%, δ ^{31}P = -1.75 to -2.78), **2+6** → **18** (85%, δ ^{31}P = -1.83 to -2.58), **3+6** → **16** (97%, δ ^{31}P = -1.71, -1.81, -1.86), **4+6** → **10** (93%, δ ^{31}P = -2.12 to -2.70) and **5+6** → **8** (90%, δ ^{31}P = -2.15 to -2.68). In a similar manner, **4** was reacted with **7** to give the protected adenosine 2′,3′-bis(O,O-bis(2-cyanoethyl)phosphate **12** (75%, δ ^{31}P= -2.95, -3.05). Complete deprotections of these fully protected blocks **8, 10, 12, 14 , 16** and **18** were carried out using standard conditions to give **9** (quantitative), **11** (65%), **13** (75%), **15** (92%), **17** (49%) and **19** (65%), respectively (see experimentals).

Conformational studies on the reference compounds 9, 11, 13, 15, 17 and 19, and their use in the structural analysis of the branched RNAs. *[A] ^{31}P-NMR studies.* Compounds **9, 11, 13, 15, 17, 19** were first studied with ^{31}P-NMR at 202 MHz. Unambiguous assignments of the ^{31}P resonances of **9, 11, 13,** and **15** were based on the two-dimensional ^{31}P-^{1}H correlation spectra, displayed in Figures 1 - 4. Table 1 lists the ^{31}P chemical shifts of the phosphate groups, as recorded at 10 °C and 80 °C. The order of the phosphate shielding is found to be δ(2'P) < δ(3'P) < δ(5'P) in each case. Furthermore, all ^{31}P resonances move downfield when the sample is heated from 10 ° to 80 °C.[7m,n] The theories on ^{31}P chemical shifts as

Table 1. ^{31}P NMR chemical shifts measured for reference compounds **9, 11, 13, 15, 17, 19** in D_2O. ^{31}P resonances were referenced against adenosine 3',5'-cyclic monophosphate (δ = 0.000 ppm) as an external reference, at the same sample temperature (ref. 21).

Compounds	10°C			80°C		
	2'P	3'P	5'P	2'P	3'P	5'P
Methyl-β-D-ribofuranosyl-2',3'-bis-ethyl phosphate (**9**)	0.93	1.40	-	1.43	1.83	-
Adenosine 2',3'-bis-ethylphosphate (**11**)	0.86	1.19	-	1.40	1.65	-
Adenosine 2',3'-bis-phosphate (**13**)	1.12	1.29	-	1.65	1.74	-
Adenosine 2',3',5'-tris-ethylphosphate (**15**)	0.73	1.09	1.68	1.37	1.66	2.32
Adenosine 2',5'-bis-ethylphosphate (**17**)	1.11	-	1.82	1.63	-	2.33
Adenosine 3',5'-bis-ethylphosphate (**19**)	-	1.47	1.65	-	2.03	2.28

developed by Gorenstein et al. provide a qualitative explanation for these observations.[22] It was concluded that stereoelectronic effects have a predominant impact on the ^{31}P chemical shift of a phosphodiester group. Therefore, phosphodiesters with *gauche-gauche* conformation (g$^-$ g$^-$, g$^-$ g$^+$, g$^+$ g$^-$, g$^+$ g$^+$) about the ζ (P-O3') and α (P-O5') bonds resonate several ppm upfield from phosphodiesters with *gauche-trans* (g$^-$ t, g$^+$ t) or *trans-gauche* (t g$^-$, t g$^+$) conformation. Structural models of reference compounds **9, 11, 13, 15, 17** and **19** clearly show that rotations around P-O5' or P-OCH_2CH_3 in the 5'-phosphate groups can easily be accommodated. On the other hand, rotation around the bridging P-O bonds in the 2'-phosphate groups is relatively difficult because of the proximate adenine base and the vicinal 3'-linked phosphate group. This is in

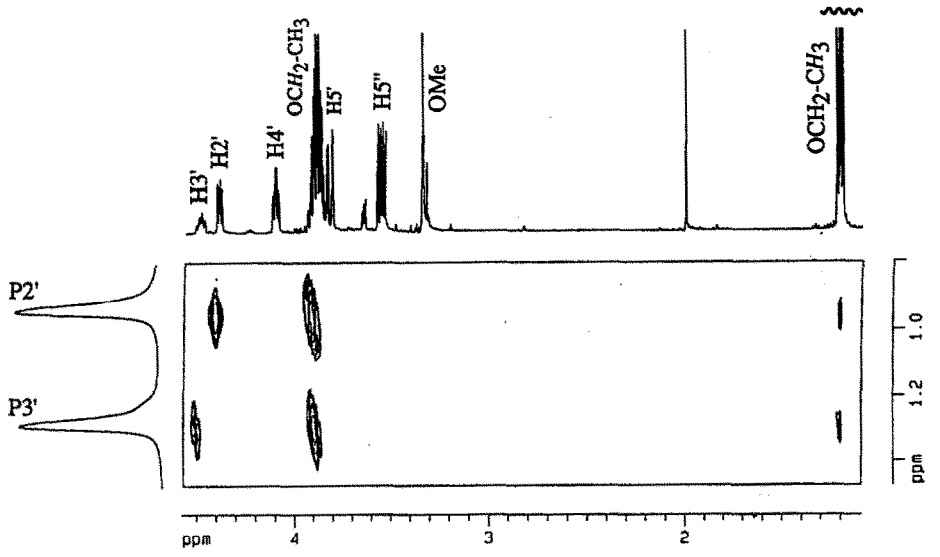

Figure 1. Two-dimensional ^{31}P-^{1}H heteronuclear correlation spectrum of compound **9** in D_2O. This spectrum was recorded in the inverse mode (absolute value) according to the method described in ref. 31. 256 Experiments of 8 scans consisting of 1K real data points were accumulated.Zero-filling to 512 real data points in the f1 dimension, and application of a sine window function in both dimensions preceded Fourier transformation.

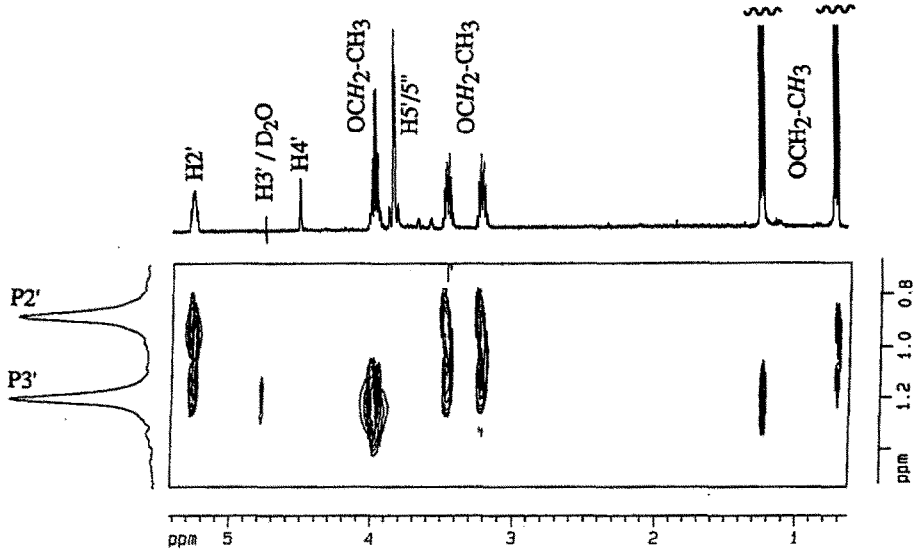

Figure 2. Two-dimensional ^{31}P-^{1}H heteronuclear correlation spectrum of compound **11** in D_2O. This spectrum was recorded as described in the legend of Figure 3, except that 40 scans were taken in each individual experiment. Note that H3' coincides with the residual HDO peak; the P3'-H3' cross peak is however clearly visible.

line with the observation that $\delta(2'P) < \delta(3'P) < \delta(5'P)$ which qualitatively implies that the population of g,g is in the following order: 2'-phosphate > 3'-phosphate > 5'-phosphate. Accordingly, heating of the sample results in downfield shifts of the 2'-, 3'- and 5'-phosphate resonances which suggests that the elevation of the sample temperature further populates the g,t and t,g rotamers. In order to assess the effect of the proximate 9-adeninyl group on the vicinal 2'- and 3'-phosphates in **11**, we have measured the chemical shifts of methyl

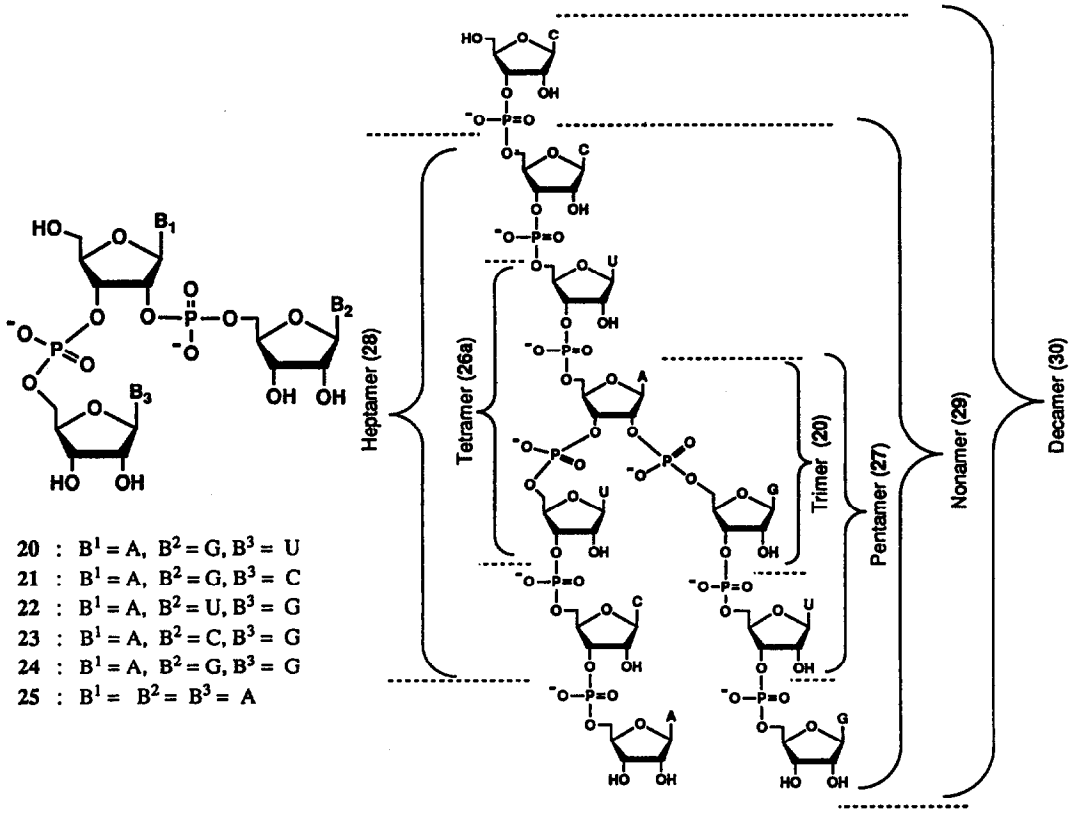

20 : $B^1 = A$, $B^2 = G$, $B^3 = U$
21 : $B^1 = A$, $B^2 = G$, $B^3 = C$
22 : $B^1 = A$, $B^2 = U$, $B^3 = G$
23 : $B^1 = A$, $B^2 = C$, $B^3 = G$
24 : $B^1 = A$, $B^2 = G$, $B^3 = G$
25 : $B^1 = B^2 = B^3 = A$

DIFFERENT SYNTHETIC MODELS 20, 26a, 27-30 FOR THE LARIAT (BRANCHED-RNA)

β-D-ribofuranosyl-2',3'-bis-phosphate **9** (Table 1). A comparison of 2'- and 3'-phosphorous chemical shifts in **9** and **11** reveals that the 9-adeninyl base has a small influence on the chemical shifts of the 2'-phosphate (upfield only by 0.07 ppm in **11** compared to **9**) while a larger effect is noted for the 3'-phosphate resonance (upfield by 0.21 ppm in **11**, compared to **9**). These observations show that the 3'-phosphate group may experience some shielding due to the ring current of the 9-adeninyl base. The shielding effect is virtually absent for the more proximate 2'-phosphate. This may be due to the fact that OMe group in **9** replaces the base in **11**, which may have a subtle inductive effect on the ^{31}P chemical shift of the 2'-linked phosphate group. *The comparison of 9 and 11 shows however, that one should be cautious in assuming that the 3'-phosphate group does not experience any shielding due to the base moiety.* [22]

The ^{31}P chemical shifts of the branched RNAs **20 - 30**, as measured at low temperature (8 - 10 °C) and high temperature (80 - 81 °C), are compiled in Table 2. Most of these data were abstracted from previous work

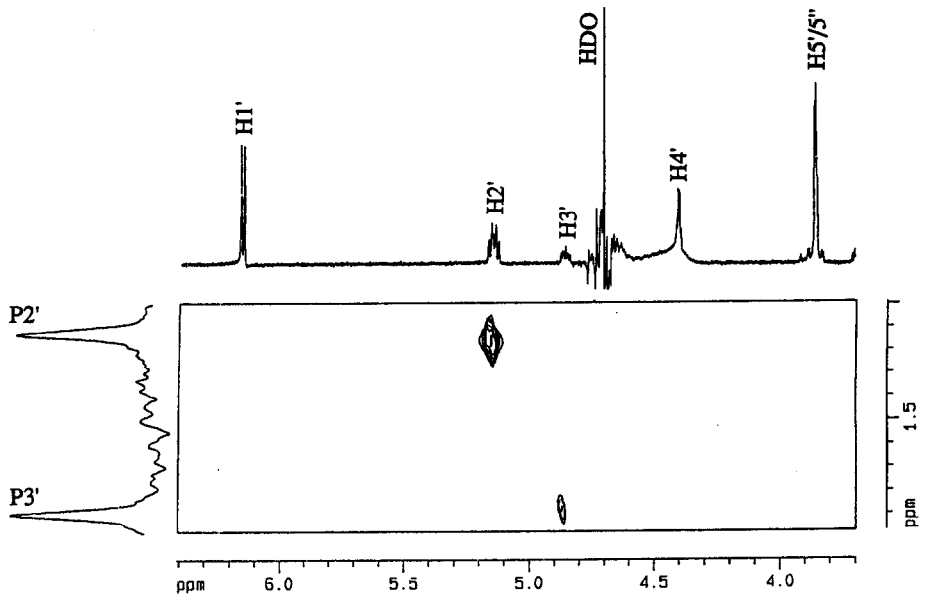

Figure 3. Two-dimensional ^{31}P-^{1}H heteronuclear correlation spectrum of compound **13** in D_2O. This spectrum was recorded as described in the legend of Figure 3, except that 16 scans were taken in each individual experiment.

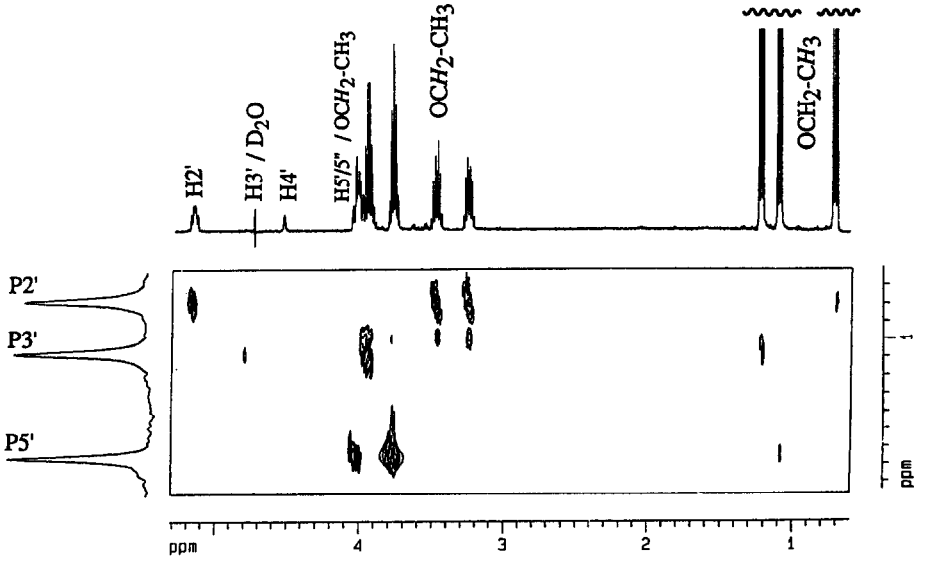

Figure 4. Two-dimensional ^{31}P-^{1}H heteronuclear correlation spectrum of compound **15** in D_2O. This spectrum was recorded as described in the legend of Figure 3, except that 40 scans were taken in each individual experiment. Note that H3' coincides with the residual HDO peak; the P3'-H3' cross peak is however clearly visible.

in this laboratory.[7m] Data on the larger model systems (**27 - 30**) are new. A selection of the data of Table 2 is incorporated in Figure 5. This graph illustrates that the structures of branched-RNA oligomers can be divided in two groups: one having predominant 2'→5' base stacking (e.g. trimers **22** and **23**, and pentamer **27**), and the other having weaker 2'→5' base stacking. Yet, the last group shows substantially stronger 2'→5' stacking than 3'→5' stacking (*vide infra*). The data in Table 2 allowed us to make two valuable comparisons. First, it is

Table 2. ^{31}P-NMR chemical shifts measured low (8 - 10 °C) and high (80 - 81 °C) temperature for branched oligonucleotides **20 - 30**. ^{31}P resonances were referenced against adenosine 3',5'-cyclic monophosphate (δ = 0.000 ppm) as an external reference, at the same sample temperature (ref. 21).

Compounds	10°C			81°C		
	2'P	3'P	5'P	2'P	3'P	5'P
$A^{2'p5'G}_{3'p5'U}$ (**20**)	0.02	0.80	-	0.61	1.11	-
$A^{2'p5'G}_{3'p5'C}$ (**21**)	0.13	0.83	-	0.63	1.15	-
$A^{2'p5'U}_{3'p5'G}$ (**22**)	-0.27	0.60	-	0.38	1.10	-
$A^{2'p5'C}_{3'p5'G}$ (**23**)	-0.34	0.62	-	0.32	1.10	-
$A^{2'p5'G}_{3'p5'G}$ (**24**)	0.06	0.73	-	0.61	1.12	-
$A^{2'p5'A}_{3'p5'A}$ (**25**)	0.14	0.62	-	0.58	1.12	-
$UA^{2'p5'G}_{3'p5'C}$ (**26**)	0.34	0.68	0.51	0.75	1.03	1.14
$UA^{2'p5'G}_{3'p5'U}$ (**26a**)	0.28	0.73	0.58	0.71	0.99	1.11
$A^{2'p5'GU}_{3'p5'UC}$ (**27**)	-0.24	0.45	-	0.31	0.75	-
$CUA^{2'p5'GU}_{3'p5'UC}$ (**28**)	0.09	0.57	0.70	0.69	a	a
$CUA^{2'p5'GUG}_{3'p5'UCA}$ (**29**)	0.15	0.60	0.67	a	a	a
$CCUA^{2'p5'GUG}_{3'p5'UCA}$ (**30**)	0.13	0.58	0.65	a	a	a
A2'→5'G	0.38	-	-	0.86	-	-
A3'→5'G	-	0.80	-	-	1.36	-

[a] could not be assigned unambiguously

seen that increasing the sample temperature results in a larger downfield shift ($\Delta\delta_{P1}$) for the 2'-phosphate than for the 3'-phosphate in trimers **20 - 25**. The $\Delta\delta_{P1}$ values are given in Table 3. *The observation that $\Delta\delta_{P1}(2') > \Delta\delta_{P1}(3')$ is a strong argument for preferred 2'→5' base stacking over 3'→5' base stacking in the trimers*, as was concluded in a previous temperature dependent ^{31}P-NMR study.[7m,n] It was also noted that the largest $\Delta\delta_{P1}$ values are found for the 2'-linked phosphates in **22** and **23**, for which the 2'-linked residue is a pyrimidine nucleoside.[7m] For tetramer **26**, it was found that $\Delta\delta_{P1}(2') \approx \Delta\delta_{P1}(3')$, which was interpreted as an indication for the occurrence of simultaneous 2'→5' and 3'→5' base stacking.[7m] At this point, it is of interest to examine the possible utility of compounds **9**, **11**, **13**, and **15** as reference compounds to determine the *oligomerization ^{31}P-NMR shifts* for branched RNAs **20 - 30**. We have applied all four standards for trimers **20 - 25**, and the resulting ^{31}P-chemical shift differences $\Delta\delta_{P2}$ to $\Delta\delta_{P5}$ are listed in Table 3. The data show that application of all four standards leads to a consistent picture for the models **20 - 25**, i.e. the result appears to be insensitive to the choice of the reference. For the remaining set of compounds (i.e. **26 - 30**), we made

only comparisons with the appropriate reference molecules, i.e. adenosine 2',3',5'-tris-(ethylphosphate) **15** for **26**, **26a**, **27** - **30**, and adenosine 2',3'-bis-(ethyl phosphate) **11** for pentamer **27**. It may be noted that the use of compound **15** leads to $\Delta\delta_{P4}$ values for the larger branched structures **28** - **30**, for which the parameter $\Delta\delta_{P1}$ could not be measured due to severe spectral overlap in the ^{31}P-NMR spectra at high temperature which prevented unambiguous assignment of the ^{31}P resonances. *This illustrates our point that use of the present*

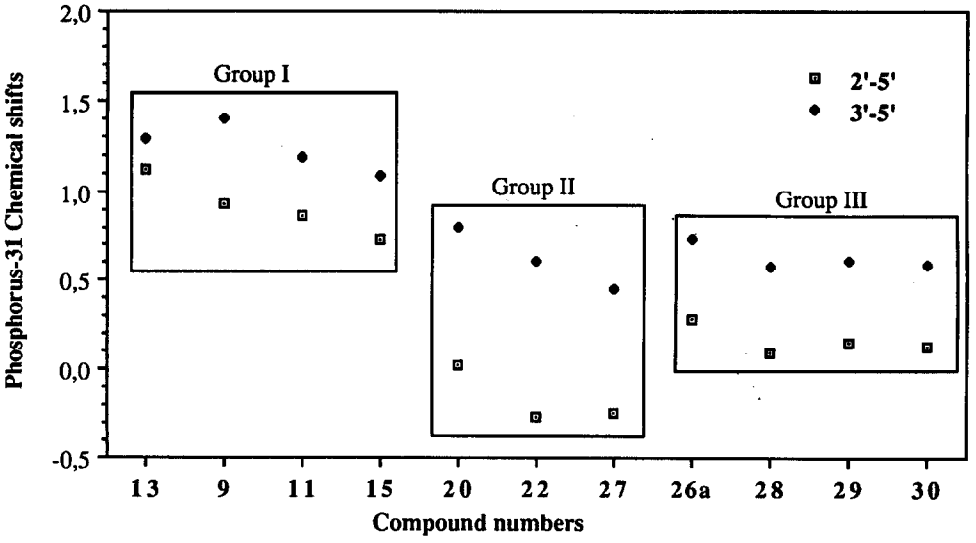

Figure 5. Plots of the ^{31}P chemical shifts for reference compounds **9**, **11**, **13**, and **15**. These reference compounds (Group I) show the most downfield chemical shifts for 2'→5' and 3'→5' phosphates indicating that tg and gt conformations are easily accessible in these compounds. Comparison of $A^{2'p5'G}_{3'p5'U}$ (**20**), $A^{2'p5'U}_{3'p5'G}$ (**22**) and $A^{2'p5'GU}_{3'p5'UC}$ (**27**) show (Group II) that the gg populations dominate in **22** and **27** more than in **20** indicating that the strength of 2'→5 stacking is in the following order in this group: (**20**) < (**22**) ≈ (**27**). Data on $CUA^{2'p5'GU}_{3'p5'UC}$ (**28**), $CUA^{2'p5'GUG}_{3'p5'UCA}$ (**29**), $CCUA^{2'p5'GUG}_{3'p5'UCA}$ (**30**) show that the relative blend of gg and (gt + tg) reaches a plateau which means that attachment of more nucleotide units is not expected to alter the nature of the 2'→5' stacked state prevalent in this group.

reference molecules can sometimes lead to structural information which is not obtainable from variable-temperature ^{31}P-NMR experiments. Use of compounds **11** and **15** as a standard for comparing ^{31}P-NMRchemical shifts may be hampered by the possible occurrence of intramolecular association between adenine and spatially close ethyl groups. This has been found in e.g. the crystal structural analysis of adenosine 5'-O-diethyl phosphate[23], and NMR data have shown that adenine-ethyl association is also possible in solution.[24] We realize that the molecular conformation of reference compound **11** may also be influenced in part by association of the adenine base and the ethyl group of the 2'-phosphate. This idea was reinforced by the observation of a relatively large chemical shift difference for the methylene protons of the ethyl group of the 2'-phosphate (-CH_2- chemical shift difference = 0.12 ppm for the ethyl group on the 2'-phosphate, and only 0.01 ppm for the ethyl group on the 3'-phosphate). Nonetheless, it is gratifying to see that there is a clear consistency between (i) use of $\Delta\delta_{P1}$ values (obtained from variable temperature ^{31}P-NMR measurements on

Table 3. Values for $\Delta\delta_{P1}$ (temperature-dependent ^{31}P NMR chemical shifts), and $\Delta\delta_{P2}$ - $\Delta\delta_{P5}$ (31P NMR oligomerization shifts) determined for the branched RNA Systems **20** - **30**. Note the general consistency that is obtained for trimers **20** - **25** by application of either temperature dependent ^{31}P NMR (leading to $\Delta\delta_{P1}$), or **9**, **11**, **13**, **15** as reference compounds (leading to $\Delta\delta_{P2}$ - $\Delta\delta_{P2}$). For the larger systems **26** - **30** we merely used the appropriate references. Note also that $\Delta\delta_{P4}$ could be determined for the larger branched systems **27** - **30**, for which attempts to measure $\Delta\delta_{P1}$ failed.

Compound	$\Delta\delta_{P1}$			$\Delta\delta_{P2}$		$\Delta\delta_{P3}$		$\Delta\delta_{P4}$			$\Delta\delta_{P5}$	
	2'P	**3'P**	**5'P**	**2'P**	**3'P**	**2'P**	**3'P**	**2'P**	**3'P**	**5'P**	**2'P**	**3'P**
$A^{2'p5'G}_{3'p5'U}$ **(20)**	0.59	0.31	-	0.84	0.39	1.10	0.49	0.71	0.29	-	0.91	0.60
$A^{2'p5'G}_{3'p5'C}$ **(21)**	0.50	0.32	-	0.73	0.36	0.99	0.46	0.60	0.26	-	0.80	0.57
$A^{2'p5'U}_{3'p5'G}$ **(22)**	0.65	0.50	-	1.13	0.59	1.39	0.69	1.00	0.49	-	1.20	0.80
$A^{2'p5'C}_{3'p5'G}$ **(23)**	0.66	0.48	-	1.20	0.57	1.46	0.67	1.07	0.47	-	1.27	0.78
$A^{2'p5'G}_{3'p5'G}$ **(24)**	0.55	0.39	-	0.80	0.46	1.06	0.56	0.67	0.36	-	0.87	0.67
$A^{2'p5'A}_{3'p5'A}$ **(25)**	0.44	0.50	-	0.72	0.57	0.98	0.67	0.59	0.47	-	0.79	0.78
$UA^{2'p5'G}_{3'p5'C}$ **(26)**	0.41	0.35	0.63					0.39	0.41	1.17		
$UA^{2'p5'G}_{3'p5'U}$ **(26a)**	0.43	0.26	0.53					0.45	0.36	1.10		
$A^{2'p5'GU}_{3'p5'UC}$ **(27)**	0.55	a	-	1.10	0.74							
$CUA^{2'p5'GU}_{3'p5'UC}$ **(28)**	0.60	a	a					0.64	0.52	0.98		
$CUA^{2'p5'GUG}_{3'p5'CUA}$ **(29)**	a	a	a					0.58	0.49	1.01		
$CCUA^{2'p5'GUG}_{3'p5'CUA}$ **(30)**	a	a	a					0.60	0.51	1.03		

$\Delta\delta_{P1} = \delta(^{31}P, 2'/3')$ at 81°C - $\delta(^{31}P, 2'/3')$ at 8 °C; $\Delta\delta_{P2} = \delta(^{31}P, 2'/3')$ in **11** (10 °C) - $\delta(^{31}P, 2'/3')$ in **20** to **26** (10 °C);

$\Delta\delta_{P3} = \delta(^{31}P, 2'/3')$ in **13** (10 °C) - $\delta(^{31}P, 2'/3')$ in **20** to **26** (10 °C); $\Delta\delta_{P4} = \delta(^{31}P, 2'/3'/5')$ in **15** (10 °C) - $\delta(^{31}P, 2'/3'/5')$ in **20** to **26** (10 °C);

$\Delta\delta_{P5} = \delta(^{31}P, 2'/3')$ in **9** (10 °C) - $\delta(^{31}P, 2'/3')$ in **20** to **26** (10 °C).

[a] Data not obtainable since ^{31}P resonances at high temperature could not be assigned unequivocally.

20 - 26 shown in Tables 2 and 3, *vide supra*) and (ii) use of $\Delta\delta_{P2}$ values (obtained by comparison with reference compound **11**). Thus, we feel that use of compound **11** as a standard is a new and independent way of identifying the preferred mode of stacking in branched RNA structures. Use of reference compound **13** has the advantage that the possibly disturbing adenine - ethyl association is eliminated. However, this is realized at the cost of incorporating *phosphomonoesters* instead of phosphodiesters in the reference system. The parameters $\Delta\delta_{P3}$, i.e. $\Delta\delta_{P3}$ = [$\delta(^{31}P, 2'/3')$ in **13**] - [$\delta(^{31}P, 2'/3')$ in **20 - 26**], are also listed in Table 3. It is clear that these data are entirely consistent with the values for $\Delta\delta_{P2}$ i.e., we see no indication of adenine-ethyl base stacking as an important determinant in the conformation of **11**. This means that reference compound **13** is also a useful standard for ^{31}P-NMR studies on branched RNA oligomers. Reference compound **15** was found to be useful for studies on larger branched RNAs, since it also provides information about the 5'-phosphate. This is demonstrated for branched-RNA **20-30** (Table 3, parameter $\Delta\delta_{P4}$, i.e. $\Delta\delta_{P4}$ = [$\delta(^{31}P, 2'/3'/5')$ in **15**] - [$\delta(^{31}P, 2'/3'/5')$ in **20 - 30**]). The $\Delta\delta_{P4}$ data are completely in line with $\Delta\delta_{P2}$ observations (*vide supra*). Of course, use of reference compound **15** is also associated with the possible danger of intramolecular adenine - ethyl association (*vide supra*). Compound **9** is a reference species in which both intramolecular base stacking and the possible occurrence of a ring current effect on the 2'- and 3'- ^{31}P resonances are eliminated. Examination of the $\Delta\delta_{P5}$ data (Table 3) i.e. $\Delta\delta_{P5}$ = [$\delta(^{31}P, 2'/3')$ in **9**] - [$\delta(^{31}P, 2'/3')$ in **20 - 26**] shows a clear consistency with respect to the use of the other standard molecules, i.e. **11**, **13**, and **15**.

[B] ^{1}H-NMR studies. Table 4 shows the ^{1}H-chemical shifts of reference compounds **9**, **11**, **13**, **15**, **17**. Table 5 compiles their $^{3}J_{HH}$ and $^{3}J_{PH}$ coupling constants measured at 20 °C and 60 °C. The J-coupling constants (Table 5) were abstracted from the one-dimensional spectra; non-first order subspectra were analyzed with the help of a computer simulation algorithm.

Table 4: ^{1}H-chemical shifts of reference compounds **9**, **11**, **13**, **15**, **17** at 20 °C using $\delta(CH_3CN)$ = 2.000 ppm as internal reference

	9	**11**	**13**	**15**	**17**	**19**
H1'	5.034	6.183	6.171	6.242	6.214	6.121
H2'	4.510	5.771	5.240	5.176	5.098	4.744
H3'	4.415	4.761	4.711	4.751	4.568	4.861
H4'	4.121	4.513	4.508	4.552	4.358	4.512
H5'	3.845	3.851	3.840	4.043	4.056	4.036
H5"	3.571	3.851	3.840	4.025	4.056	4.036
H2 (Me in **9**)	3.358	8.718	8.202	8.198	8.226	8.207
H8		8.311	8.322	8.445	8.439	8.423

The ribose ring conformations were analyzed in terms of a rapid South-type (C2'-*endo*) / North-type (C3'-*endo*) equilibrium. We used the program PSEUROT, and the couplings $J_{1'2'}$, $J_{2'3'}$, and $J_{3'4'}$ as experimental input values. The results of these analyses (Table 5) clearly show that the ribose rings in **11**, **13**, **15**, **17** and **19** preferentially adopt a South type conformation, but it is predominantly North type in **9**. This difference in sugar conformation in **9** from the rest (**11**, **13**, **15**, **17** and **19**) can be most probably attributed to the anomeric effect. The coupling constants $J_{4'5'}$ and $J_{4'5''}$ were used to analyze the conformation of the C4'-C5' backbone bond. For this, we used the equation: $\%(\gamma^+) = 100 \times (13.3 - \Sigma) / 9.7$, with $\Sigma = J_{4'5'} + J_{4'5''}$.[1c] It is found that γ^+ is predominant, except in **9** (Table 5). For compounds **15**, **17**, or **19** which bear a phosphate group on the 5'-terminus, it was also possible to examine the conformation around the C5'-O5' (β) bond. For

Table 5. ^{1}H NMR Data Measured for Compounds **9, 11, 13, 15, 17 & 19**. Coupling Constants are Given in Hz.
Calculated Conformational Populations of the South type (C2'-endo) Puckered Ribose Ring, and the Rotamers γ^+ (C4'-C5') and β^t (C5'-O5')

Compound	Temp (°C)	$J_{1'2'}$	$J_{2'3'}$	$J_{3'4'}$	$J_{4'5'}$	$J_{4'5''}$	$J_{2'P2'}$	$J_{3'P3'}$	$J_{5'P5'}$	$J_{5'P5''}$	$^4J_{2'P3'}$	x(South)	%(γ^+)	%(βt)
9	20	1.2	5.0	7.2	3.6	6.3	8.6	8.6	--	--	--	10	12	--
	60	1.7	5.1	7.0	3.1	6.3	8.4	8.5	--	--	--	15	18	--
11	20	7.7	4.9	2.5	2.7	3.3	9.8	7.4	--	--	1.5	91	75	--
	60	7.7	5.0	1.7	2.7	3.6	9.9	7.6	--	--	1.4	95	72	--
13	20	7.5	4.7	2.6	2.9	3.0	9.8	7.4	--	--	1.0	94	76	--
	60	7.4	4.7	2.8	3.1	3.3	9.9	7.4	--	--	1.0	92	75	--
15	20	7.4	5.2	1.8	2.5	3.6	9.9	8.0	x	x	1.3	95	74	x
	60	7.0	5.0	2.1	3.6	3.8	9.6	7.7	3.8	4.1	1.4	90	61	85
17	20	6.3	5.2	2.8	3.8	3.8	9.2	--	4.2	4.5	--	82	59	80
	60	6.3	5.2	3.4	3.6	3.8	8.8	--	3.3	4.1	--	77	61	87
19	20	6.9	4.9	2.7	2.9	3.0	--	7.8	4.0	4.2	0.6	85	76	83
	60	6.3	5.1	3.1	3.0	3.8	--	7.5	3.6	4.4	0.8	78	67	84

this, we used the formula: % β^t = 100 x (23.9 - Σ') / 18.9, with $\Sigma' = J_{5'p} + J_{5''p}$.[1c] These results (Table 5) clearly show that β^t is the predominant rotamer in **15**, **17**, and **19**, which is also completely in line with available data on other 5'-nucleotides. As a complement to our previous studies on base stacking in branched RNA oligomers, we have now determined the oligomerization shift (designated as $\Delta\delta_1$) (see Table 6) of the base protons H2A (branch-point), H5U (3'-linked nucleotide), and H8G (2'-linked nucleotide) in the series **20**, **26a**, **27 - 30**. The residues A (branch point), U (3'-linked nucleotide) and G (2'-linked nucleotide) are a constant structural motif in the series **20**, **26a**, **27 - 30**. The data in Table 6 also allow comparison with other related branched and linear RNA oligomers. It is well known that H2A and H5 of U or C can serve as valuable probes for studies on base stacking, especially when a purine base, having a relatively strong ring current, is located in a proximate position in the stack.[1] Use of H8A/G or H6U/C is more dangerous, since the conformation around the glycosidic bond also influences the H8 or H6 chemical shifts. In order to assess the relative 2'→5' versus 3'→5' stackings in the branched RNAs, we have considered both the oligomerization shift of H2A, H5U and H8G ($\Delta\delta_1$) at 20 °C (Table 6) and at 40 °C (data not shown due to the analogous trend) and the temperature-dependent change of δ(H2A), δ(H5U) and δ(H8G) in the range 10 - 80 °C ($\Delta\delta_2$) (Table 6). A perusal of $\Delta\delta_1$H2A and $\Delta\delta_1$H8G in A3'p5'G ($\Delta\delta_1$H2A = 0.114 & $\Delta\delta_1$H8G = 0.258) and A2'p5'G ($\Delta\delta_1$H2A = 0.392 & $\Delta\delta_1$H8G = 0.459) clearly shows that the mutual diamagnetic shielding of guanine residue by the adenine and vice versa is stronger in A2'p5'G suggesting a stronger base-base stacked interaction in the latter. Now, a comparison of $\Delta\delta_1$H2A and $\Delta\delta_1$H8G in A2'p5'G with those of $A^{2'p5'G}_{3'p5'U}$ (**20**) ($\Delta\delta_1$H2A = 0.420 & $\Delta\delta_1$H8G = 0.450) and $A^{2'p5'GU}_{3'p5'UC}$ (**27**) ($\Delta\delta_1$H2A = 0.513 & $\Delta\delta_1$H8G = 0.499) shows that they belong to the same category of A2'→5'G base-stacked conformation, while the family of $UA^{2'p5'G}_{3'p5'U}$ (**26a**) ($\Delta\delta_1$H2A = 0.219 & $\Delta\delta_1$H8G = 0.433), $CUA^{2'p5'GU}_{3'p5'UC}$ (**28**) ($\Delta\delta_1$H2A = 0.260 & $\Delta\delta_1$H8G = 0.453), $CUA^{2'p5'GUG}_{3'p5'UCA}$ (**29**) ($\Delta\delta_1$H2A = 0.305 & $\Delta\delta_1$H8G = 0.471), $CCUA^{2'p5'GUG}_{3'p5'UCA}$ (**30**) ($\Delta\delta_1$H2A = 0.296 & $\Delta\delta_1$H8G = 0.460) belong to a slightly different type. Note that the $\Delta\delta_1$H5(5'-pU) in $A^{2'p5'G}_{3'p5'U}$ (**20**), $A^{2'p5'GU}_{3'p5'UC}$ (**27**), $UA^{2'p5'G}_{3'p5'U}$ (**26a**), $CUA^{2'p5'GU}_{3'p5'UC}$ (**28**), $CUA^{2'p5'GUG}_{3'p5'UCA}$ (**29**), $CCUA^{2'p5'GUG}_{3'p5'UCA}$ (**30**) are respectively 0.113, 0.064, 0.143, 0.062, 0.163, and 0.176 ppm. In conjunction with the above data, an examination of $\Delta\delta_1$H2A and $\Delta\delta_1$H5(5'-pU or pC) in A3'p5'U ($\Delta\delta_1$H2A = 0.005 & $\Delta\delta_1$H5U = 0.354) shows that (i) the diamagnetic shielding of H5 of 5'-pU residue by the branch-point A in all of these oligomeric branch-RNA is rather small compared to what is found in A3'p5'U, and (ii) the diamagnetic shielding of H8G of 2'-pG residue is at least as high as in A2'p5'G, (iii) the observed high diamagnetic shielding of H2A is therefore expected to arise from the 2'-pG residue. Furthermore, it may be noted that in $A_{3'p5'}U$ and $U_{3'p5'}A_{3'p5'}U$ has a $\Delta\delta_1$H5(5'-pU) = 0.354[26] and 0.252 ppm[27], respectively, showing the reduced 5'pU stacking with A in the latter due to 5'-conformatiuonal transmission.[30] The parameters $\Delta\delta_1$H5(U3'p) are found to be 0.153 and 0.293 ppm in $U_{3'p5'}A$ and $U_{3'p5'}A_{3'p5'}U$, respectively, compared to those of the counterparts in $UA^{2'p5'G}_{3'p5'U}$ (**26a**) ($\Delta\delta_1$H5(U3'p) = 0.115 ppm and $\Delta\delta_1$H5(5'-pU) = 0.064 ppm). This clearly shows that both U3'p and 5'-pU are involved in the stacked interaction with central adenine residue in $U_{3'p5'}A_{3'p5'}U$[27], while these interactions along the 3'→5' axis are much less important in $UA^{2'p5'G}_{3'p5'U}$ (**26a**). *In fact, above comparison*

Table 6: Use of different markers to probe intramolecular base stacking in the branched RNA oligomers **20** -**24** (trimers), **26, 26a** (tetramers), **27** (pentamer), **28** (heptamer), **29** (nonamer) and **30** (decamer). The markers used H2A of the branch-point, H5 of 3'-linked pyrimidine and H8G of 2'-linked guanosine. Data on some dimers and a linear trimer are included for comparison (Note: variation of δ at 20°C from 2-5 mM concentration is less than 0.05 ppm (see for e. g., ref. 25).

Oligomers (Concentration)	δH2A (20 °C)	$\Delta\delta_1$H2A[a] (20 °C)	$\Delta\delta_2$H2A[d]	δH5(pU/pC) (20 °C)	$\Delta\delta_1$H5Py[a] (20 °C)	$\Delta\delta_2$H5Py[d]	δH8G (20 °C)	$\Delta\delta_1$H8G[a] (20 °C)	$\Delta\delta_2$H8G[d]	δH5(Up) (20 °C)	$\Delta\delta_1$H5U[a] (20 °C)
$A^{2'p5'G}_{3'p5'U}$ **20** (4 mM)	7.798	0.420[b]	0.211	5.782	0.113[e]	0.047	7.662	0.450[f]	0.047	–	–
$UA^{2'p5'G}_{3'p5'U}$ **26a** (5 mM)	7.979	0.219[c]	0.124	5.831	0.064[e]	–0.006	7.679	0.433[f]	0.029	5.745	0.115[i]
$A^{2'p5'GU}_{3'p5'UC}$ **27** (4 mM)	7.705	0.513[b]	0.200	5.752	0.143[e]	0.032	7.613	0.499[f]	0.086	–	–
$CUA^{2'p5'GU}_{3'p5'UC}$ **28** (3 mM)	7.938	0.260[c]	0.077	5.833	0.062[e]	–0.012	7.659	0.453[f]	0.030	5.741	0.119[i]
$CUA^{2'p5'GUG}_{3'p5'UCA}$ **29** (2 mM)	7.893	0.305[c]	0.121	5.732	0.163[e]	n	7.641	0.471[f]	0.005	5.732	0.128[i]
$CCUA^{2'p5'GUG}_{3'p5'UCA}$ **30** (2 mM)	7.902	0.296[c]	0.102	5.719	0.176[e]	n	7.650	0.460[f]	0.004	5.697	0.163[i]
$A^{2'p5'G}_{3'p5'C}$ **21** (4 mM)	7.807	0.411[b]	0.207	5.889	0.180[j]	0.084	7.673	0.439[f]	0.046	–	–
$A^{2'p5'U}_{3'p5'G}$ **22** (5 mM)	7.952	0.266[b]	0.165	5.596	0.299[e]	0.070	7.974	0.138[f]	0.015	–	–
$A^{2'p5'C}_{3'p5'G}$ **23** (5 mM)	7.874	0.344[b]	0.188	5.698	0.371[j]	0.074	7.980	0.132[f]	0.02	–	–
$A^{2'p5'G}_{3'p5'G}$ **24** (5 mM)	7.763	0.455[b]	0.252	–	–	–	7.618[m]	0.494[m,f]	0.052[m]	–	–
$UA^{2'p5'G}_{3'p5'C}$ **26** (5 mM)	7.958	0.240[c]	0.124	5.880	0.189[j]	0.101	7.697	0.415[f]	0.018	5.726	0.134[i]
U3'p5'A3'p5'U (5 mM)	8.167	0.031[l]	–	5.643	0.252[e]	–	–	–	–	5.567	0.293[i]
A3'p5'U (4 mM)	8.126	0.005[g]	–	5.531	0.354[e]	–	–	–	–	–	–
A3'p5'C (10-30 mM)	8.031	0.090[g]		5.620	0.449[j]	–	–	–	–	–	–
A2'p5'G (5 mM)	7.809	0.392[k]	0.188	–	–	–	7.653	0.459[f]	0.039	–	–
A3'p5'G (5 mM)	8.007	0.114[g]	–	–	–	–	7.854	0.258[f]	–	–	–
U3'p5'A (10-30 mM)	8.180	0.018[h]	–	–	–	–			–	5.707	0.153[i]

[a] $\Delta\delta_1$ = oligomerization shift at 20°C = [δ(monomer) - δ(oligomer)], $\Delta\delta_1$H2A at 40°C showed an analogous trend; [b] referenced to **11** (δH2A = 8.218); [c] referenced to **15** (δH2A = 8.198); [d] $\Delta\delta_2$ = δ (80 °C) - δ(10 °C); [e] referenced to 5'-UMP (δH5U = 5.895); [f] referenced to 5'-GMP (δH8G = 8.112); [g] referenced to 3'-AMP (δH2A = 8.121); [h] referenced to 5'-AMP (δH2A = 8.199); [i] referenced to 3'-UMP (δH5U = 5.860); [j] referenced to 5'-CMP (δH5C = 6.069); [k] referenced to **17** (δH2A = 8.201); [l] referenced to **19** (δH2A = 8.198); [m] 2'-linked residue. Data on nucleoside monophosphates and dimers A3'p5'C and U3'p5'A were abstracted from ref 26. Data on U3'p5'A3'p5'U were abstracted from ref. 27. [n] Could not be determined due to spectral overlap at 80 °C.

shows that both U3'→5'A and A3'→5'U stacking are weakest in 26a compared to U3'p5'A, A3'p5'U and U3'p5'A3'p5'U. It may be noted that for $UA^{2'p5'G}_{3'p5'C}$ (**26**), it is found that $\Delta\delta_1$H5(5'pC) = 0.189 ppm (compare $\Delta\delta_1$H5(5'pC) = 0.449 ppm in A3'p5'C), which may indicate that some A3'→5'C stacking occurs in **26**.

[C] ^{13}C-NMR studies. Compounds **9**, **11**, **13**, **15**, **17**, and **19** have been studied with ^{13}C-NMR at 125.7 MHz. Our main interest was to determine the three-bond carbon-phosphorus coupling constants $^3J_{P3'-C4'}$, $^3J_{P3'-C2'}$, $^3J_{P2'-C1'}$, and $^3J_{P2'-C3'}$, which contain information about the conformation around the bonds O3'-C3' (ε), and O2'-C2' (ε'). These data are summarized in Table 7. The Newman projections of the staggered rotamers around ε and ε' are shown in Figure 2. Molecular models clearly indicate that the occurrence of the ε^+ and ε'^+ rotamers can be disregarded safely, since highly unfavorable steric interactions are encountered in these conformations.[7p,9a] Therefore, it has become customary to treat the C3'-O3' conformation as a two-state ε^- / ε^t equilibrium, and, analogously, the C2'-O2' conformation as an ε'^- / ε'^t equilibrium (Figure 6). The Newman projections around C3'-O3' show that three vicinal coupling constants contain information about the ε-conformation: $^3J_{P3'-C4'}$, $^3J_{P3'-C2'}$, $^3J_{P3'-H3'}$. The relationship between torsion angles POCC, POCH and coupling constants are expressed in the following Karplus equations[28]:

$$^3J_{P3'C4'} = 6.9\cos^2(\phi) - 3.4\cos(\phi) + 0.7$$
$$^3J_{P3'C2'} = 6.9\cos^2(\phi - 120) - 3.4\cos(\phi - 120) + 0.7$$
$$^3J_{P3'H3'} = 15.3\cos^2(\phi + 120) - 6.1\cos(\phi + 120) + 1.6 \quad [\text{where, } \phi = [\text{P-O-C3'-C4'}].$$

Note that trigonal symmetry for the location of C2', C4', and H3' with respect to the C3'-O3' bond is assumed. Values for $^3J_{P3'-C2'}$, $^3J_{P3'-H3'}$ can be calculated for any combination of $\phi(\varepsilon^t)$, $\phi(\varepsilon^-)$, and $x(\varepsilon^-)$. For each set of $\phi(\varepsilon^t)$, $\phi(\varepsilon^-)$, and $x(\varepsilon^-)$, a root mean square (r.m.s.) error can be calculated, identifying the agreement between the calculated and experimental values for $^3J_{P3'-C4'}$, $^3J_{P3'-C2'}$, $^3J_{P3'-H3'}$. Table 8 compiles the estimated regions of $\phi(\varepsilon^t)$, $\phi(\varepsilon^-)$, and $x(\varepsilon^-)$, which showed best agreement with the experimental results (minimal r.m.s. error). The data in Table 8 clearly show that ε^- is preferred over ε^t for compounds **9**, **11**, **13**, **15**, trimer **20**, and tetramer **26** (%(ε^t) ranges from 14 ± 6 % to 40 ± 20 %). It is noted that compounds **9**, **11**, **13**, **15**, and trimer **20** show very comparable data with respect to the ε conformational analysis. This

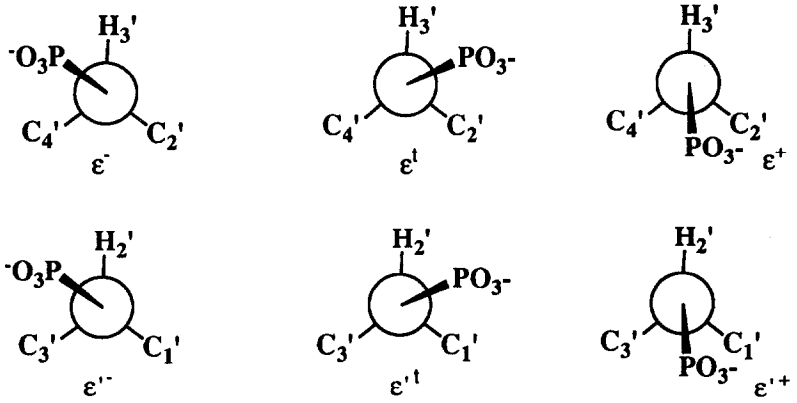

Figure 6 : Newman projections along the O3'-C3' bond (upper row), the O2'-C2' bond (lower row) of the branch-point adenosine

Table 7. ^{13}C NMR Data Measured on Compounds **1 - 5**, and Results from Best-Fit Analyses with Respect to Conformational Analysis of the C3'-O3' (ε) Bond.

Compound	Temperature (°C)	$^3J_{P2'C1'}$	$^3J_{P2'C3'}$	$^3J_{P3'C2'}$	$^3J_{P3'C4'}$	$^3J_{P2'H2'}$	$^3J_{P3'H3'}$
Methyl-β-D-ribofuranosyl-bis-2',3'-ethyl phosphate (**9**)	20	5.5	3.7	6.9	0.8	9.6	7.5
Adenosine bis-2',3'-ethyl phosphate (**11**)	20	5.6	3.8	6.8	0.6	9.8	7.4
	60	5.2	4.0	6.2	0.6	9.9	7.6
Adenosine bis-2',3'-phosphate (**13**)	20	5.4	5.2	6.6	0.8	9.8	7.4
	60	5.4	5.2	6.4	0.8	9.9	7.4
Adenosine tris-2',3'-5'-ethyl phosphate (**15**)	20	4.8	4.6	6.2	0.8	4.8	8.0
	60	4.4	4.8	6.2	1.2	5.0	7.7
Adenosine bis-2',5'-ethyl phosphate (**17**)	20	5.8	3.6	--	--	5.0	--
	60	6.2	3.4	--	--	4.8	--
Adenosine bis-3',5'-ethyl phosphate (**19**)	20	--	--	5.2	3.2	--	7.8
	60	--	--	5.2	3.6	--	7.5
$A^{2'p5'G}_{3'p5'U}$ (**20**)	27	7.6	3.0	6.6	< 1	8.6	7.9
	45	7.2	4.2	6.7	< 1	9.1	7.6
$UA^{2'p5'G}_{3'p5'C}$ (**26**)	27	2.8	5.6	4.6	2.0	9.0	8.1
	45	4.8	5.2	5.2	2.5	9.0	8.3

strengthens our idea that compounds **9, 11, 13, 15** are useful reference systems for conformational studies on trimeric branched RNAs. The ε-conformational analysis on tetramer **26** seems to indicate that rotamer ε^- is less populated in comparison with compounds **9, 11, 13, 15** and trimer **20**. Also, the ε-conformational analysesare quite consistent with respect to the values for $\phi(\varepsilon^t)$ and $\phi(\varepsilon^-)$; $\phi(\varepsilon^t)$ is around 205°, and $\phi(\varepsilon^-)$ is around 270°, which is in favourable agreement with literature data. Additional evidence for a preferred ε^- conformation in **9, 11, 13, 15** and trimer **20** was provided by the fact that a small four-bond J-coupling (0.5-1.5 Hz) is observed between P3' and H2' in these compounds, but not in **19** and **26**. Such a four-bond coupling strongly indicates a planar W-type arrangement of the coupling path P3'-O3'-C3'-C2'-H2', i.e. a high population of the conformational combination ε^- (C3'-O3') and a South (C2'-*endo*) puckered ribose ring. An analogous approach was used for the analysis of the conformation around the C2'-O2' (ε') bond. The vicinal coupling constants are now : $^3J_{P2'-C3'}$, $^3J_{P2'-C1'}$, $^3J_{P2'-H2'}$ which we used in the Karplus equations[28]:

$$^3J_{P2'C3'} = 6.9\cos^2(\phi') - 3.4\cos(\phi') + 0.7$$
$$^3J_{P2'C1'} = 6.9\cos^2(\phi' - 120) - 3.4\cos(\phi' - 120) + 0.7$$
$$^3J_{P2'H2'} = 15.3\cos^2(\phi' + 120) - 6.1\cos(\phi' + 120) + 1.6 \text{ [where, } \phi' = \text{[P2'-O2'-C2'-C3']}.$$

Again it is assumed that there is a trigonal symmetry for the location of C1', C3' and H2'. The results of the r.m.s. calculations concerning the C2'-O2' bond are also given in Table 8. The results indicate that ε'^- domi-

Table 8: C3'-O3' (ε) and C2'-O2' (ε') torsional angles of **9, 11, 13, 15 ,17, 19, 20** and **26**.

	2'p				3'p			
Compound	ε'^t	ε'^-	% ε'^t	RMS	ε^t	ε^-	% ε^t	RMS
9	210±15	260±5	32±10	0.18	200±20	270±5	14±10	0.76
11	221±10	258±5	33±10	0.29	210±20	270±5	14±10	0.89
13	218±10	261±10	48±20	0.75	204±20	271±5	18±10	0.89
15	195±15	285±15	50±5	0.53	202±20	266±5	13±10	0.95
17	185±30	285±15	41±10	0.50	–	–	–	–
19	–	–	–	–	205±20	272±15	40±20	0.44
20	219±10	269±5	25±10	0.56	208±20	268±5	14±10	0.81
26	220±5	272±20	75±15	0.24	205±20	265±10	31±15	1.09

nates over ε'^t in the case of compound **9, 11** and trimer **20**, while ε'^t dominates over ε'^- for the tetramer **26**. Rotamers ε'^- and ε'^t have roughly equal populations for the remaining compounds (i.e. **13, 15,** and **17**). The results in Table 8 led us to the following tentative conclusions: (i) the ε- rotamer around the C3'-O3' bond is predominant for compounds **9, 11, 13, 15** and trimer **20**. This conformational preference is thus an intrinsic property of the 2',3' vicinal phosphate moiety, and not a reflection of base stacking. Diminished preferences for ε^- are found for **19** (in which the 2'-phosphate group is removed as compared to **15**) and tetramer **26**. (ii) The ε^- rotamer around C2'-O2' is preferred for compound **9** and **11**, and trimer **20**, but this is less clear for compounds **13, 15,** and **17**. Tetramer **26** definitely shows a preference for ε^t around the C2'-O2' bond.

[D] Molecular modelling of the branched trimer $A^{2'p5'G}_{3'p5'U}$ *(**20**) based on the NMR data.* Energy minimizations using the AMBER program[29] (version 3.0A) were performed on several starting geometries based on the NMR-data.[7p] From ^{1}H-NMR coupling constants in combination with the program PSEUROT the starting sugar conformations were determined for adenosine (P = 162°, Φ_m = 38°, X_S = 74%), guanosine (P = 0°, Φ_m = 38°, or P = 143°, Φ_m = 41°, X_S = 56%) and for uridine (P = -15°, Φ_m = 36°, or P = 149°, Φ_m = 37°, X_S = 59%). The endocyclic torsional angles were then calculated from the P and Φ_m values.[7p] Based on

ROESY-experiments the glycosidic bond torsions were set to *syn* (χ = 45°) for adenosine and *anti* (χ = -150°) for guanosine and uridine.[7p] Analysis of the ^{31}P-^{13}C and ^{31}P-^{1}H coupling constants showed a preference for ε^- (C3'-O3') and ε'^- (C2'-O2') conformations (*vide supra*). For all three residues it was found that the γ^+-rotamer is preferred, and for the uridine and guanosine residues the β^t-rotamer predominates.[7p]

Table 9: AMBER calculations on $A^{2'p5'G}_{3'p5'U}$ **(20)**, starting structures were constructed based on our NMR spectroscopic data (see text)

	Energy minimized conformation (Fig. 3)					
	Structure I (E = -7.22 kcal/mol)			Structure II (E = -7.17 kcal/mol)		
	A	G	U	A	G	U
ν_0	-34.4	-4.1	-21.5	-34.6	-6.5	-23.2
ν_1	43.6	-20.8	34.1	43.4	-19.1	35.9
ν_2	-35.1	35.3	-32.8	-34.4	34.7	-34.1
ν_3	16.4	-39.4	21.7	15.6	-40.2	22.1
ν_4	11.1	27.7	-0.4	11.6	29.7	0.5
P	146.1	24.9	161.7	145.0	28.2	160.3
Φ_m	43.4	40.0	35.6	43.1	40.5	37.3
χ	45.1	-157.8	-159.1	42.8	-157.3	-161.8
α	-	-66.5	-59.4	-	-73.6	-176.6
β	-	175.8	-176.4	-	179.2	-172.5
γ	55.5	59.8	64.8	57.7	59.3	56.2
δ	139.1	80.9	145.8	138.4	79.7	145.9
δ^* [a]	-155.9	-81.0	-152.6	-153.6	-81.7	-153.8
ε	-82.5	-	-	-77.4	-	-
ε'	-94.4	-	-	-99.0	-	-
ζ	-74.6	-	-	-76.9	-	-
ζ'	-75.7	-	-	-67.0	-	-

[a] δ^* = [C4'-C3'-C2'-O2']

Several conformers were generated based (i) on S or N sugar conformation for G and U, (ii) both ζ and α for the 2'-phosphate were set to -60°. It was realized that only $g^-(\zeta)$,$g^-(\alpha)$ conformation for the 2'-phosphate can yield an A2''5'G stacked structure in agreement with the observed ^{1}H-NMR chemical shifts. ^{31}P-NMR chemical shifts also support a conformation with a relatively high contribution of $g^-(\zeta)$,$g^-(\alpha)$ for the 2'-phosphate. (iii) The sugar of A was set to South. (iv) ζ and α for the 3'-phosphate group were set to -60°, +60° or 180°. (v) γ and β for all residues were set to 60° and 180° respectively. These 36 structures were then energy minimized by AMBER. Inspection of the molecular energies shows that two structures (designated as I and II in Table 9) are preferred over the others. Structures I and II have a virtually equal stability (E(I) = -7.22, and E(II) = -7.17 kcal/mol; the next-lowest energy structure has E = -5.63 kcal/mol). The torsion angles describing the geometries of structures I and II are listed in Table 9, and both structures are displayed in Figure 7. The most important difference between structures I and II is the conformation of the 3'-phosphate group, which is $g^-(\zeta)$,$g^-(\alpha)$ for I, and $g^-(\zeta)$,$t(\alpha)$ for II. Both models show A2'→5'G stacking, while the U-base is not involved in stacking. These geometries explain the experimental spectroscopic data.

CONCLUSIONS

The present systematic compilation of the ^{31}P chemical shifts of the branch-point 2'→5' and 3'→5'-linked vicinal phosphate groups shows that $\delta^{31}P(2') < \delta^{31}P(3')$ for all branched RNA oligomers studied in

this work. This implies that a g(ζ),g(α) conformation is more dominant in the 2'-phosphates than in the 3'-phosphates. The obvious explanation for these findings is that 2'→5' stacking prevails over 3'→5' stacking around the branch-point. Model building studies revealed that 2'→5' stacking is compatible only with g⁻(ζ),g⁻(α) conformation of the 2'-phosphate group. On the other hand, AMBER calculations along with ^{31}P-

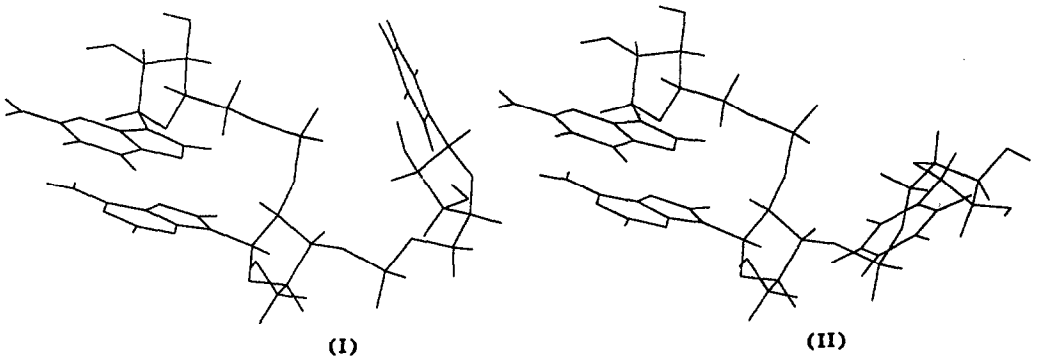

Figure 7. Structures I and II, as calculated with the AMBER program. The 3'-phosphate group has g⁻(ζ),g⁻(α) conformation in structure I, and g⁻(ζ)t(α) conformation in structure II (see text).

NMR data show that the 3'-phosphate group has a higher population of g⁻(ζ),t(α) conformers. The largestpopulation of g⁻(ζ),g⁻(α) in the 2'-phosphate group is encountered in trimers **22** and **23**, and pentamer **27** (Tables 2 and 6, Figure 1). It is important to note that ^{31}P-NMR was used in two respects: (i) comparisons of δ(^{31}P) values with the appropriate reference compounds, leading to ^{31}P-NMR oligomerization shifts, and (ii) temperature dependent ^{31}P-NMR measurements. Both approaches consistently led to the above conclusions. Use of ^{1}H-NMR oligomerization shifts ($\Delta\delta_1$ estimated against an appropriate reference compound as described in the footnote of Table 6), and the data from variable temperature ^{1}H-NMR experiments ($\Delta\delta_2$, Table 6) are mutually consistent: relatively high values for $\Delta\delta_1$ are usually accompanied by relatively high values for $\Delta\delta_2$. Notable exceptions to this are the unnatural trimers **22** and **23** (Table 6), for which relatively high values of $\Delta\delta_1$(H5 5'-pU) are accompanied by low values for $\Delta\delta_2$(H5 5'-pU). Apparently, this is because elevation of the sample temperature from 20 to 80 °C hardly diminished 2'→5' base stacking in these compounds. Compilation of the $\Delta\delta_1$ and $\Delta\delta_2$ values (Table 6) provided ample support for the conclusions based on ^{31}P-NMR. We wish to emphasize that compounds **20, 26a, 27 - 30** feature A2'→5'G rather than A3'→5'U base stacking. We feel that this conclusion is of special importance since

Table 10 : Relative strength of 2'→ 5' stacking versus 3'→ 5' stacking in the naturally occurring branched-RNAs

Relative strength of stacking	$A^{2'p5'G}_{3'p5'U}$ (**20**)	$UA^{2'p5'G}_{3'p5'U}$ (**26a**)	$A^{2'p5'GU}_{3'p5'UC}$ (**27**)	$CUA^{2'p5'GU}_{3'p5'UC}$ (**28**)	$CUA^{2'p5'GUG}_{3'p5'UCA}$ (**29**)	$CCUA^{2'p5'GUG}_{3'p5'UCA}$ (**30**)
2'→ 5'stacking	++	+	++	+	+	+
3'→ 5'stacking	~0	~0	~0	~0	~0	~0

structures **27** - **30** can be regarded as representative models for the biologically occurring lariat structure. Table 10 summarizes the conclusions with regard to 2'→5' and 3'→5' stacking in **20**, **26a**, **27** - **30**. Interestingly, removal of the 5'-linked uridine, as in trimer **20** and pentamer **27**, leads to *stronger* A2'→5'G stacking. This means that 5'-linked uridine residue *makes a choice* as regards its participation in the stacked interactions along the 2'→5' or the 3'→5' axis. Our present study clearly shows that it *prefers* to promote a " 5'-conformational transmission effect" along the 2'→5' leg over the 3'→5' in the branched-RNAs **20**, **26a**, **27** - **30** compared to the linear 3'→5'-linked oligo-RNAs such as in AUA, AAUA, UAUA,[30] and UAU[27] in which such " 5'-conformational transmission effect" can only be dictated along the 3'→5' axis.

EXPERIMENTAL

^{1}H-NMR spectra were recorded in δ scale with Jeol FX 90 Q and Bruker AMX-500 spectrometers at 90 and 500 MHz respectively, using TMS or H_2O (set at 4.7 ppm) as internal standards. ^{31}P-NMR spectra were recorded at 36 and 202 MHz in the same solvent using 85 % phosphoric acid or cAMP (for compounds described in Tables 1- 3)as external standard. TLC was carried out using pre-coated silica gel F_{254} plates in the dichloromethane-methanol mixture: (A) 90: 10 (v/v). Dry pyridine was obtained by successive distillations over CaH_2 and 4-toluenesulfonyl chloride. Acetonitrile was distilled from P_2O_5 under argon. Dimethylformamide was distilled over CaH. The column chromatographic separations of all the protected intermediates were carried out using Merck G 60 silica gel. Preparative thin layer separations were carried out using pre-coated silica gel F_{254} plates (200 x 200 x 2 mm) and DEAE-Sephadex A-25 from Pharmacia was used for the ion exchange chromatography for the deprotected materials

5'-O-Fluorenmethoxycarbonyl-β-methyl-D-ribofuranoside (5). A mixture of α/β-methyl-D-ribofuranoside (~ 25:75 ratio) (250 mg, 1.52 mmol) was coevaporated with dry pyridine and redissolved in dry pyridine (15 ml). Fluorenmethoxycarbonylchloride (511 mg, 1.98 mmol) was dissolved in dry dichloromethane (15 ml) in a dropping funnel. The pyridine solution was cooled to 0 °C and then the dichloromethane solution was added dropwise over 3 h. After complete addition the reaction mixture was stirred for another half hour at 0 °C. The reaction mixture was poured into ammonium bicarbonate solution and extracted with dichloromethane (3 x 50 ml). Silica column chromatography (1% EtOH/ 0.5% pyridine in CH_2Cl_2) yielded 132 mg (30%, calc. from 75% - content of β-isomer in the starting mixture) of **5**. R_f (A): 0.55; ^{1}H-NMR ($CDCl_3$): 7.82-7.21 (m, 8H) arom.; 4.86 (s, 1H) H-1'; 4.49-4.01 (m, 8H) H-2', H-3', H-4', -5', -5''& -$CHCH_2$- of fluorenmethoxy-; 3.34 (s, 3H) -OCH_3; 2.82 (br, 2H) 2 x OH;

5'-O-Fluorenmethoxycarbonyl-β-methyl-D-ribofuranoside-2',3'-bis(O-(2-cyanoethyl)-O-ethyl phosphate) (8). Phosphoramidite reagent **6** (257 mg, 1.04 mmol, 10 eq) was weighed into a dry 25 ml round bottom flask and dry 15 % dimethylformamide / acetonitrile solution (3.5 ml, 0.9 mmol tetrazole / ml) was added under argon (argon balloon). Then dry and sublimed tetrazole (218 mg,3.11 mmol, 30 eq) was added under stirring and it rapidly went into solution followed by a quick formation of a precipitate. After 3 min stirring dry solid **5** (40 mg, 0.104 mmol, 1 eq) was added to the colorless suspension and the clear reaction solution was then stirred for 40 min at room temperature under argon. 0.1 M I_2 / tetrahydrofuran / pyridine / H_2O (7:2:1 v/v/v) (11 ml) was added and the reaction solution was stirred for 15 min and was then poured into 0.1 M sodium thiosulfate / concentrated ammonium bicarbonate solution and extracted with dichloromethane (3 x 50 ml). The pyridine-free gum obtained after toluene co-evaporation of the organic residue was then purified by short silica gel column chromatography (0-5 % EtOH in CH_2Cl_2, in(40 mg, 0.104 mmol, 1 eq) 1 % increments) to finally give the title compound as a white powder after co-evaporation with toluene and cyclohexane (66 mg, 90%). R_f (A): 0.64; ^{1}H-NMR ($CDCl_3$): 7.82-7.21 (m, 8H) arom.; 5.05-4.71 (m, 3H) H-1', H-2'& H-3'; 4.58-4.05 (m, 14H) H-4', -5', -5'', -$CHCH_2$- of fluorenmethoxy-, 2 x -OCH_2CH_3 & 2 x -OCH_2CH_2CN; 3.36 (s, 3H) -OCH_3; 2.81 (m, 4H) 2 x -OCH_2CH_2CN; 1.38 (m, 6H) 2 x -OCH_2CH_3; ^{31}P-NMR ($CDCl_3$): -2.15, -2.25, -2.39, -2.46, -2.51, -2.63, -2.68 ppm.

6-N-Benzoyl-5'-O-(4,4'-dimethoxy)trityladenosine 2',3'-bis(O-(2-cyanoethyl)-O-ethyl phosphate) (10). **4** (200 mg, 0.297 mmol, 1 eq) was treated with **6** (734 mg, 2.97 mmol, 10 eq) and tetrazole (624 mg, 8.91 mmol, 30 eq) in a corresponding way as for preparation of **8** and the intermediary 2',3'-bisphosphitetriester was oxidized with iodine solution (31 ml). **10** was isolated by silica gel chromatography. (274 mg, 93%). R_f (A): 0.55; ^{1}H-NMR ($CDCl_3$+2,6-lutidine): 9.33 (br, 1H) NH; 8.69 (s,

1H) H-8; 8.26 (s, 1H) H-2; 8.04-6.76 (m, 18H) arom.; 6.37 (d, $J_{1',2'}$= 5.85Hz, 1H) H-1'; 5.89 (m, 1H) H-2'; 5.33 (m, 1H) H-3'; 4.49 (m, 1H) H-4'; 4.34-3.91 (m, 8H) 2 x -O*CH*$_2$CH$_2$CN & 2 x -O*CH*$_2$CH$_3$; 3.76 (s, 6H) 2 x -OCH$_3$; 3.53 (m, 2H) H-5',-5''; 2.84-2.62 (m, 4H) 2 x -OCH$_2$*CH*$_2$CN; 1.52-1.07 (m, 6H) 2 x -OCH$_2$*CH*$_3$; ^{31}P-NMR ($CDCl_3$+2,6-lutidine) : -2.12, -2.19, -2.31, -2.44, -2.56, -2.61, -2.70 ppm.

6-N-benzoyl-5'-O-(4,4'-dimethoxy)trityladenosine-2',3'-bis(O,O-di(2-cyanoethyl) phosphate) (12). **4** (100 mg, 0.149 mmol, 1 eq) was treated with **7** (368 mg, 1.49 mmol, 10 eq) and tetrazole (312 mg, 4.46 mmol, 30 eq) of in a corresponding way as for preparation of **8** and the intermediary 2',3'-bisphosphitetriester was oxidized with iodine solution (15.6 ml). **12** was isolated by silica gel chromatography (112 mg, 75%). R_f (A): 0.45; ^{1}H-NMR ($CDCl_3$+2,6-lutidine): 9.07 (br, 1H) NH; 8.72 (s, 1H) H-8; 8.24 (s, 1H) H-2; 8.08-6.77 (m, 18H) arom.; 6.39 (d, $J_{1',2'}$= 7.10Hz, 1H) H-1'; 5.89 (m, 1H) H-2'; 5.42 (m, 1H) H-3'; 4.52-4.01 (m, 11H) H-4',-5',-5''& 4x-O*CH*$_2$CH$_2$CN; 3.78 (s, 6H) 2 x -OCH$_3$; 3.57 (m,2H) H-5',5'';2.84-2.60 (m,4H) 4 x -OCH$_2$*CH*$_2$CN; ^{31}P-NMR ($CDCl_3$+2,6-lutidine): -2.95,-3.05 ppm.

6-N-benzoyladenosine 2',3',5'-tris(O-(2-cyanoethyl)-O-ethylphosphate) (14). Dry solid 6-N-benzoyladenosine (**1**) (150 mg, 0.404 mmol, 1 eq) was treated with **6** (1.5g, 6.05 mmol, 15 eq) and tetrazole (1.27g, 18.16 mmol, 45 eq) in 40% dimethylformamide / acetonitrile in a corresponding way as for preparation of **8** and the intermediary 2',3'-bisphosphitetriester was oxidized with iodine solution (65 ml). **14** was isolated by silica gel chromatography. (277 mg, 80%). R_f (A): 0.40; ^{1}H-NMR ($CDCl_3$): 8.67 (s, 1H) H-8; 8.27 (s, 1H) H-2; 7.98-7.39 (m, 5H) arom.; 6.28 (d, $J_{1',2'}$= 4.64Hz, 1H) H-1'; 5.63 (m, 1H) H-2'; 5.35 (m, 1H) H-3'; 4.53-3.87 (m, 15H) H-4', -5', -5'', 3 x -O*CH*$_2$CH$_2$CN & 3 x -O*CH*$_2$CH$_3$; 2.83-2.60 (m, 6H) 3 x -OCH$_2$*CH*$_2$CN; 1.41-1.04 (m, 9H) 3 x -OCH$_2$*CH*$_3$; ^{31}P-NMR ($CDCl_3$): -1.75, -1.81, -1.93, -2.22, -2.27, -2.32, -2.37, -2.44, -2.51, -2.64, -2.69, -2.73, -2.78 ppm.

6-N-benzoyl-3'-O-t-butyldimethylsilyladenosine-2',5'-bis(O-(2-cyanoethyl)-O-ethyl phosphate) (16). **3** (30 mg, 0.062 mmol, 1eq) was treated with **6** (153 mg, 0.62 mmol, 10 eq) and tetrazole (130 mg, 1.86 mmol, 30 eq) in a corresponding way as for preparation of **8** and the intermediary 2',5'-bisphosphitetriester was oxidized with iodine solution (6.5 ml). **16** was isolated by silica gel chromatography.(49 mg, 97%). R_f (A): 0.49; ^{1}H-NMR ($CDCl_3$): 8.80, 8.79 (2 x s, 1H) H-8; 8.35, 8.33 (2 x s, 1H) H-2; 8.05-7.46 (m, 5H) arom.; 6.32 (d, $J_{1',2'}$= 4.40Hz, 1H) H-1'; 5.46 (m, 1H) H-2'; 4.78 (m, 1H) H-3'; 4.36-3.83 (m, 11H) H-4', -5', -5'', 2 x -O*CH*$_2$CH$_2$CN & 2 x -O*CH*$_2$CH$_3$; 2.78-2.61 (m, 4H) 2 x -OCH$_2$*CH*$_2$CN; 1.37-1.17 (m, 6H) 2 x -OCH$_2$*CH*$_3$; 0.92 (s, 9H) t-butylSi-; 0.16 (s, 6H) 2 x CH$_3$Si-; ^{31}P-NMR ($CDCl_3$): -1.71, -1.81, -1.86 ppm.

6-N-benzoyl-2'-O-pixyladenosine 3',5'-bis(O-(2-cyanoethyl)-O-ethylphosphate) (18). **2** (63 mg, 0.1 mmol, 1 eq) was treated with **6** (247 mg, 1 mmol, 10 eq) and tetrazole (210 mg, 3 mmol, 30 eq) in a corresponding way as for preparation of **8** and the intermediary 3',5'-bisphosphitetriester was oxidized with 11 ml of iodine solution. **18** was isolated by silica gel chromatography (80 mg, 85%). R_f (A): 0.54; ^{1}H-NMR ($CDCl_3$+2,6-lutidine): 9.09 (br, 1H) NH; 8.62 (s, 1H) H-8; 8.12-6.26 (m, 19H) arom.& H-2; 6.03 (d, $J_{1',2'}$= 7.57Hz, 1H) H-1'; 5.17 (m, 1H) H-2'; 4.60-3.99 (m, 12H) H-3',-4', -5', -5'', 2 x -O*CH*$_2$CH$_2$CN & 2 x -O*CH*$_2$CH$_3$; 2.89-2.62 (m, 4H) 2 x -OCH$_2$*CH*$_2$CN; 1.53-1.20 (m, 6H) 2 x -OCH$_2$*CH*$_3$; ^{31}P-NMR ($CDCl_3$+2,6-lutidine): -1.83, -1.88, - 2.00, -2.12, -2.49, -2.58 ppm.

Deprotection of compound 8. **8** (66 mg, 0.093 mmol) was treated with concentrated aqueous NH_3 (25 ml) for 16 h at room temperature. After evaporation of the solvents the residue was dissolved in water/dichloromethane.The water phase was extracted in a Falcon tube three times with dichloromoethane.The water phase was transferred to a round flask and evaporated. The material was sodium exchanged by elution through a Dowex column (1 x 20 cm, Na^+ form) with distilled water. The collected water solution was evaporated and the residue was lyophilized from distilled water. The aqueous phase was evaporated to dryness to give 33 mg (quantitative) of **9**. ^{31}P-NMR (D_2O): -0.05, -0.34 ppm.

Deprotection of compound 10. Concentrated aqueous NH_3 (40 ml) was added to compound **10** (274 mg, 0.275 mmol) in a 100 ml flask and distilled dioxane was pipetted to the mixture until a clear solution emerged. After stirring for 24 h at room temperature the solvents were removed by evaporation and the residue coevaporated once with water. The residue was dissolved in aqueous 80% acetic acid (30 ml) and stirred for 20 min at room temperature. After evaporation and co-evaporation with distilled water the residue was dissolved in of distilled water (20 ml) and extracted with diethylether in a Falcon tube. The residue was redissolved in distilled water (3 ml) and the solution was applied onto four preparative TLC plates and the plates were eluted with a acetonitrile/water (4:1 v/v) solution. The appropriate band was collected from each plate and the material washed off by filtration from the silica with distilled water. The combined water solution was evaporated and the residue was redissolved in distilled water and centrifuged. The supernatant was loaded onto a short DEAE-Sephadex A-25 column (4 x 3 cm, HCO_3^- form) and the column was eluted with a linear gradient 0.001 - 0.005M (200 ml/200 ml), 0.005 - 0.10M (200 ml/200 ml), 0.10 - 0.2M (200 ml/200 ml) ammonium bicarbonate solution, pH 7.5. The appropriate fractions were pooled, evaporated and co-evaporated with

distilled water a few times to remove the salt. The material obtained was sodium exchanged in the same way as for **9** to give **11** (85 mg, 65%, as Na^+ form after Dowex H^+ exchange) . ^{31}P-NMR (D_2O): -0.37, -0.68 ppm.

Deprotection of compound 12. 12 (112 mg, 0.112 mmol) of was treated with concentrated aqueous NH_3 (50 ml) for 26 h at 55 °C followed by treatment with aqueous 80% acetic acid (30 ml) in the same way as described for **10**. Acetonitrile/water (2:1 v/v) was used as eluent for preparative TLC purification. A linear gradient [0.001 - 0.005M (200 ml/200 ml), 0.005 - 0.2M (200 ml/200 ml), 0.2 - 0.4M (200 ml/200 ml)] of ammonium bicarbonate solution (pH 7.5) was used for the DEAE- Sephadex A-25 purification to give **13**. (43 mg, 75% as Na^+ form after Dowex H^+ exchange). ^{31}P-NMR (D_2O): +1.73, +1.00 ppm.

Deprotection of compound 14. 14 (277 mg, 0.323 mmol) was treated with concentrated aqueous NH_3 (40 ml) in the same way as for **10**. Acetonitrile/water (3:1 v/v) was used as eluent for preparative TLC purification. A linear gradient [0.001 - 0.005M (200 ml/200 ml), 0.005 - 0.15M (200 ml/200 ml), 0.15 - 0.3M (200 ml/200 ml)] of ammonium bicarbonate solution (pH7.5) was used for the DEAE-Sephadex A-25 purification to give **15** (197 mg, 92% as Na^+ form after Dowex H^+ exchange). ^{31}P-NMR (D_2O): +0.32, -0.29, -0.66 ppm.

Deprotection of compound 16. 16 (49 mg,0.061 mmol) was treated with concentrated aqueous NH_3 in the same way as for **10**. The residue obtained after the evaporations was dissolved in distilled tetrahydrofuran (1 ml) and 320 µl 1M TBAF x $3H_2O$ (5 eq.) in tetrahydrofuran was added and stirred for 20 h at room temperature. The reaction solution was evaporated and dissolved in a small amount of water and applied to preparative TLC as for **10**. Acetonitrile/water (4:1 v/v) was used as eluent. A gradient 0.001 - 0.005M (200 ml/200 ml), 0.005 - 0.1M (200 ml/200 ml), 0.1 - 0.2M (200 ml/200 ml) ammonium bicarbonate solution, pH 7.5 was used for the DEAE- Sephadex A-25 purification to give **17** (26 mg, 49% as Na^+ form after Dowex H^+ exchange). ^{31}P-NMR (D_2O): +0.37, -0.39 ppm.

Deprotection of compound 18. 18 (80 mg, 0.085 mmol) was treated with concentrated aqueous NH_3 (40 ml) followed by treatment with aqueous 80% acetic acid (30 ml) in the same way as for **10**. Acetonitrile/water (4:1 v/v) was used as eluent for preparative TLC purification. A gradient 0.001 - 0.005M (200 ml/200 ml), 0.005 - 0.1M (200 ml/200 ml), 0.1 - 0.2M (200 ml/200 ml) ammonium bicarbonate solution, pH 7.5 was used for the DEAE-Sephadex A-25 purification to give of **19** (49 mg, 65%, as Na^+ form after Dowex H^+ exchange). ^{31}P-NMR (D_2O): +0.22, 0.00 ppm.

ACKNOWLEDGEMENTS

Authors thank Swedish Board for Technical Development, Swedish Natural Science Research Council for generous financial supports and Wallenbergstiftelsen, Forskningsrådsnämnden (FRN) and University of Uppsala for funds for the purchase of a 500 MHz Bruker AMX NMR spectrometer. Financial Support from the European Molecular Biology Organization (EMBO) through two-year EMBO fellowship to LHK is gratefully acknowledged.

REFERENCES

1. (a) Cantor, C.R.; Schimmel, P.R. *Biophysical Chemistry*; *Vols. 1 - 3*; Freeman: San Francisco. 1980. (b) Saenger, W. *Principles of Nucleic Acid Structure*; Springer Verlag: New York. 1983. (c) Altona, C. *Recl. Trav. Chim. Pays-Bas* . **1982**, *101*, 413.
2. Ts'o, P.O.P. *Basic Principles in Nucleic Acid Chemistry* ; Academic Press: New York. 1974.
3. Shefter, E.; Barlow, M.; Sparks, R. A.; Trueblood, K. N.*Acta Crystallogr.* **1969**, *B25*, 895.
4. Krishnan, R.; Seshadri, T. P.; Viswamitra, M.*Nucl. Acids Res.* **1991**,*19*, 370.
5. Parthasarathy, R.; Malik, M.; Fridey, S. M. *Proc. Natl. Acad. Sci. USA* .**1982**,*79*, 7292.
6. (a) Doornbos, J.; den Hartog, J. A. J.; van Boom, J. H.; Altona, C. *Eur. J. Biochem*..**1981**,*116*, 403. (b) Ts'o, P. O. P.; Kondo, N. S.; Schweizer, M. P.; Hollis, D. P. *Biochemistry* . **1969**, *8*, 997.
7. Our work on synthesis and conformational analysis of brached RNA oligomers is published in: (a) Vial, J-M.; Balgobin, N.; Remaud, G.; Nyilas, A.; Chattopadhyaya, J.*Nucleosides & Nucleotides*. **1987**, *6* (1&2), 209. (b) Zhou, X-X.; Nyilas, A.; Remaud, G.; Chattopadhyaya, J.*Tetrahedron*. **1987**, *43*, 4685. (c) Remaud, G.; Vial, J-M.; Nyilas, A.; Balgobin, N.; Chattopadhyaya, J.*Tetrahedron*. **1987**, *43*, 947. (d) Földesi, A.; Balgobin, N.; Chattopadhyaya, J.*Tetrahedron Lett*. **1989**, *30*, 881.(e) Zhou, X-X.; Nyilas, A.; Remaud, G.; Chattopadhyaya, J.*Tetrahedron*. **1987**, *43*, 4685. (f) Balgobin, N.; Földesi, A.; Remaud, G.; Chattopadhyaya, J.*Tetrahedron*. **1988**, *44*, 6929. (g) Zhou, X-X.; Remaud, G.; Chattopadhyaya, J.*Tetrahedron*. **1988**, *44*, 6471. (h) Sund, C.; Földesi, A.; Yamakage, S-N.; Agback,

P.; Chattopadhyaya, J.*Tetrahedron*. **1991**, *47*, 6305. (i) Vial, J-M.; Remaud, G.; Balgobin, N.; Chattopadhyaya, J.*Tetrahedron*. **1987**, *43*, 3997. (j) Koole, L. H.; Balgobin, N.; Buck, H. M.; Kuijpers, W.; Nyilas, A.; Remaud, G.; Chattopadhyaya, J. *Recl. Trav. Chim. Pays-Bas*. **1988**, *107*, 663. (k) Zhou, X-X.; Nyilas, A.; Remaud, G.; Chattopadhyaya, J.*Tetrahedron*. **1988**, *44*, 571. (l) Sandström, A.; Balgobin, N.; Nyilas, A.; Remaud, G.; Vial, J-M.; Zhou, X-X.; Chattopadhyaya, J. *Nucleosides & Nucleotides*. **1988**, *7* , 827. (m) Sandström, A.; Remaud, G.; Vial, J-M.; Zhou, X-X.; Nyilas, A.; Balgobin, N.; Chattopadhyaya, J. *J. Chem. Soc., Chem. Comm*. **1988**, 542. (n) Remaud, G.; Balgobin, N.; Sandström, A.; Koole, L. H.; Drake, A. F.; Vial, J-M.; Zhou, X-X.; Buck, H. M.; Chattopadhyaya, J. *J. Biochemical & Biophysical Methods*. **1989**, *18*, 1. (o) Remaud, G.; Balgobin, N.; Glemarec, C.; Chattopadhyaya, J. *Tetrahedron*. **1989**, *45*, 1537. (p) Glemarec, C.; Jaseja, M.; Sandström, A.; Koole, L. H.; Agback, P.; Chattopadhyaya, J. *Tetrahedron*. **1991**, *47*, 3417. (q) Koole, L.H.; Remaud, G.; Zhou, X-X.; Buck, H. M.; Chattopadhyaya, J. *J. Chem. Soc., Chem. Comm*. **1989**, p.859-861. (r) Remaud, G.; Vial, J-M.; Balgobin, N.; Koole, L. H.; Sandström, A.; Drake, A. F.; Zhou, X-X.; Glemarec, C.; Chattopadhyaya, J. *Structure and Methods, Volume 3, DNA & RNA* ; Sarma, R. H.; Sarma, M. H. Eds. Adenine Press: New York, 1990; pp. 319 - 337. (s) Koole, L. H.; Agback, P.; Glemarec, C.; Zhou, X-X.; Chattopadhyaya, J.*Tetrahedron* . **1991**, *47*, 3183.

8. Recently, the first circular model of the lariat RNA structure has been synthesized in our laboratory: Sund, C.; Agback, P.; Chattopadhyaya, J.*Tetrahedron*. (submitted).
9. (a) Damha, M. J.; Ogilvie, K. K. *Biochemistry* . **1988**, *27*, 6403. (b) Lee, M.; Huss, S.; Gosselin, G.; J Imbach, J-L.; Hartley, J. A.; Lown, J. W. *J. Biomol. Struct. Dyns*. **1987**, *5*, 651.
10. Hayakawa, Y.; Noheri, T.; Noyori, R.; Imai, J.*Tetrahedron Lett*. **1987**, *28*, 2623.
11. Damha, M. J.; Ogilvie, K. K. *J. Org. Chem*. **1988**, *53*, 3710.
12. Remaud, G.; Zhou, X-X.; Öberg, B.; Chattopadhyaya, J. *Reviews of Heteroatom Chemistry*; MYU Publishing Inc.: Tokyo, 1987, pp. 340-366.
13. Yoshikawa, M.; Kato, T. *Bull. Chem. Soc. Japan*. **1967**, *40*, 2849.
14. Takaku, H.; Shimada, Y.; Oka, H. *Chem. Pharm. Bull*. **1973**, *21*, 1844.
15. Moffat, J. G.; Khorana, H. G. *J. Am. Chem. Soc*. **1961**, *83*, 663.
16. Hayakawa, Y.; Wakabayashi, S.; Nobori, T.; Noyori, R.*Tetrahedron Lett*. **1987**, *28*, 2259.
17. Bannwarth, W.; Trzeciak, A. *Helv. Chim. Acta* . **1987**, *70*, 175.
18. Perich, J. W.; Johns, R. B. *Synthesis*. **1988**, 142.
19. Reese, C. B.; Yau, L. *J. Chem. Soc., Chem. Comm*. **1978**, 1050.
20. Smrt, J. *Tetrahedron Lett*. **1973**, *47*, 4727.
21. Haasnoot, C. A. G.; Altona, C. *Nucl. Acids Res*. **1979**, *6*, 1135.
22. (a) Gorenstein, D. G. *Jerusalem Symposium, NMR in Molecular Biology*; Reidel: Dordrecht, Netherlands. 1978; pp. 1-15. (b) Gorenstein, D. G. *Phosphorus-31 NMR: Principles and Applications* ; Academic Press: New York. 1984. (c) Gorenstein, D. G. *Chem. Rev*. **1987**, *87*, 1047.
23. Brennan, R. G.; Kondo, N. S.; Sundaralingam, M. *J. Am Chem. Soc*. **1984**, *106*, 5671.
24. Kan, L. S.; Barrett, J. C.; Miller, P. S.; Ts'o, P. O. P. *Biopolymers* . **1973**, *12*, 2225.
25. (a) Hartel, A. J.; Lankhorst, P. P.; Altona, C. *Eur J. Biochem*.**1982**, *129*, 343. (b) Mellema, J. R.; van der Woerd, R.; van der Marel, G. A.; van Boom, J. H.; Altona, C. *Nucl. Acids Res*. **1984**, *12*, 5061.
26. (a) Lee, C.-H.; Ezra, F. S.; Kondo, N. S.; Sarma, R. H.; Danyluk, S. S. *Biochemistry* **1976**, *15*, 3627. (b) Ezra, F. S.; Lee, C.-H.; Kondo, N. S.; Danyluk, S. S.; Sarma, R. H. *Biochemistry* . **1977**, *16*, 1977.
27. Lee, C.-H.; Tinoco, Jr., I. *Biophys. Chem*. **1980**, *11*, 283.
28. Lankhorst, P. P.; Haasnoot, C. A. G.; Erkelens, C.; Altona, C. *J. Biomol. Struct. Dyns*. **1984**, *1*, 1387.
29. Weiner, S. J.; Kollman, P. A.; Nguyen, D. T.; Case, D. A. *J. Comput. Chem*. **1986**, *7*, 230.
30. (a) van den Hoogen, Y. Th.; Treurniet, S. J.; Roelen, H. C. P. F.; de Vroom, E.; van der Marel, G. A.; van Boom, J. H.; Altona, C. *Eur. J. Biochem*. **1988**, *171*, 155. (b) van den Hoogen, Y. Th. *PhD. Thesis;* Leiden University, Netherlands. 1988. Note that A stands for 6-N,N-dimethylaminoadenosine.
31. Bax, A.; Griffey, R. H.; Hawkins, B. L*J. Magn. Res*. **1983**, *55*, 301.